

## CHAPTER 3. RESULTS OF FIELD AND LABORATORY INVESTIGATIONS

This chapter presents the data from laboratory and field investigations on the studied pavements, as collected by the research team. This data will be analyzed and discussed in detail in the following chapters. Section 3.1 gives an overview of each test site, with accompanying site photos. Detailed field evaluations including distress surveys are available in appendix A. Section 3.2 gives a description and petrographic overview of each concrete. Additional microphotographs and petrographic discussions are found in appendix B. Finally, laboratory results for each of the concrete properties measured in this study are presented in section 3.3.

### 3.1 Field Test Sites

The LTPP database was started in 1987 with the goal of determining ways to increase pavement service life through improvements in design, construction and maintenance practices. By investigating the performance of inservice pavement sections, specific information can be obtained on the various factors and design features that most influence pavement deterioration. In this project the intent was to use the LTPP database on JPCP's (from the GPS-3 database) that are 10 years in age or older, which had exhibited low-distress performance. Major study variables consisted of a range of ages, levels of distress and strength, and climates.

Because a large pool of high strength older pavements was not available, the primary selection criteria were good performing pavements of varying strength levels, with service lives greater than their original design life of 20 to 25 years, located in different climates. A total of 15 pavement sections were selected for study. (Sections 13-GA1-5 and 13-GA1-6 are considered as one section for most discussions. They differ in that 13-GA1-5 rests of a cement treated base while 13-GA1-6 is on an asphalt treated base. Their performance is similar).

Figure 3.1.1 depicts graphically the ages and cumulative traffic volumes in ESAL's for each of the studied test sections. Table 3.1.1 lists key pavement system information for the selected sections. The table includes site information obtained from both the LTPP database and field testing from this study. Ten of the fifteen JPCP's are on CTB's, and that the majority are undoweled. It is noteworthy that the Iowa section 19-3055 and the Wisconsin section 55-3008 have no subbase, and this design feature and the low California Bearing Ratio (CBR) subgrade at those sites have a major effect on faulting.

The PCC slab thicknesses are nearly constant for the tested sites, with average value of 237 mm (9.3 in). The largest slab thickness, 297 mm (11.7 in), was found on the thickened slab section of the experimental test road 06-7456 on I-5 near Tracy,

California. Figure 3.1.2 shows the pavement layer thicknesses of the concrete slab, base and subbase layers for each test section.

The environmental data for the selected sites are shown in table 3.1.2. It is noteworthy that the California pavements are in a mild climate with low freeze index. Consequently, the combined effects from freeze-thaw cycles and deicing salts on PCC durability at joints are not a problem in California.

The investigated test sites are presented in the following sections. First, six test sections from the dry-no-freeze (DNF) region; one test section from the dry-freeze (DF) region; then five test sections from the wet-freeze (WF) region; and finally three test sections from the wet-no-freeze (WNF) region are presented. The general locations of the test sections are shown in figure 3.1.3. Along with the brief site description, a few photographs have been selected to show the overall pavement condition.

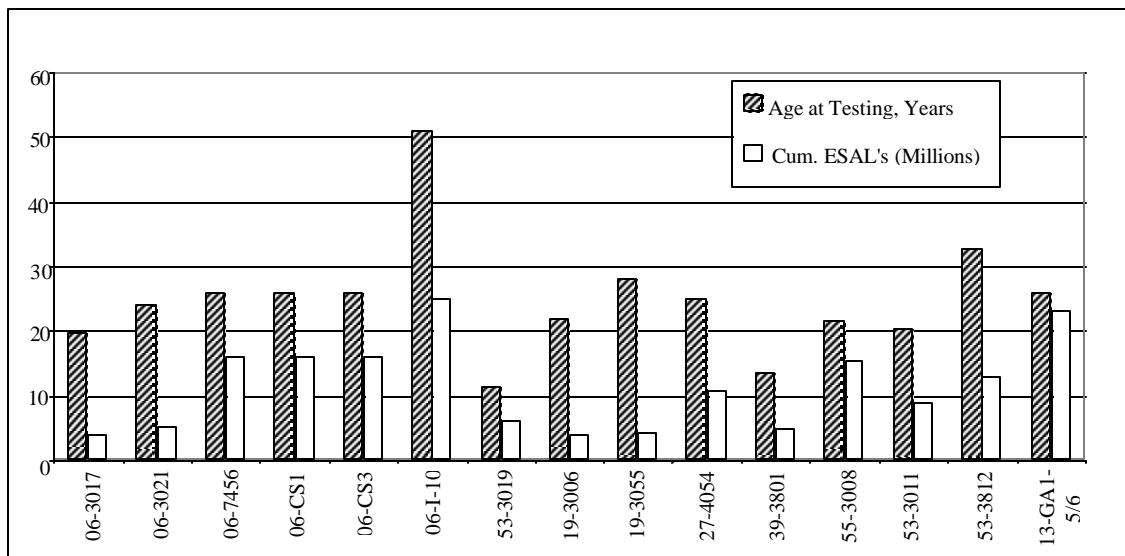


**Figure 3.1.1** Years in service and estimated cumulative ESAL's (millions) for the selected test sections.

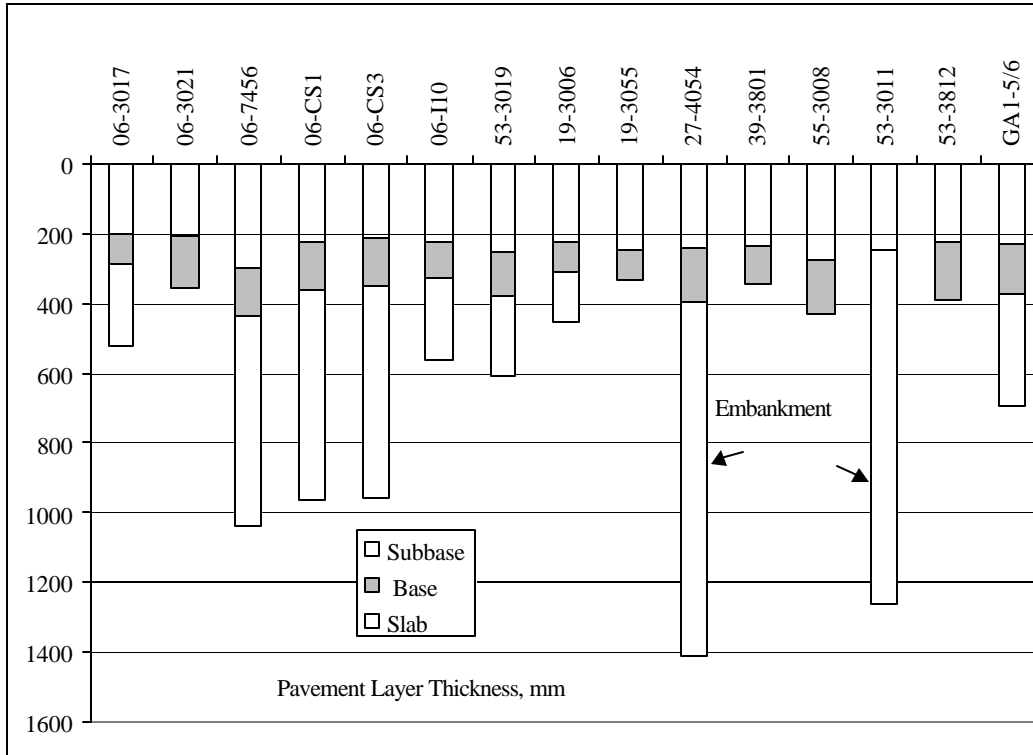


Figure 3.1.2 Pavement layer thickness for the studied pavements (mm).

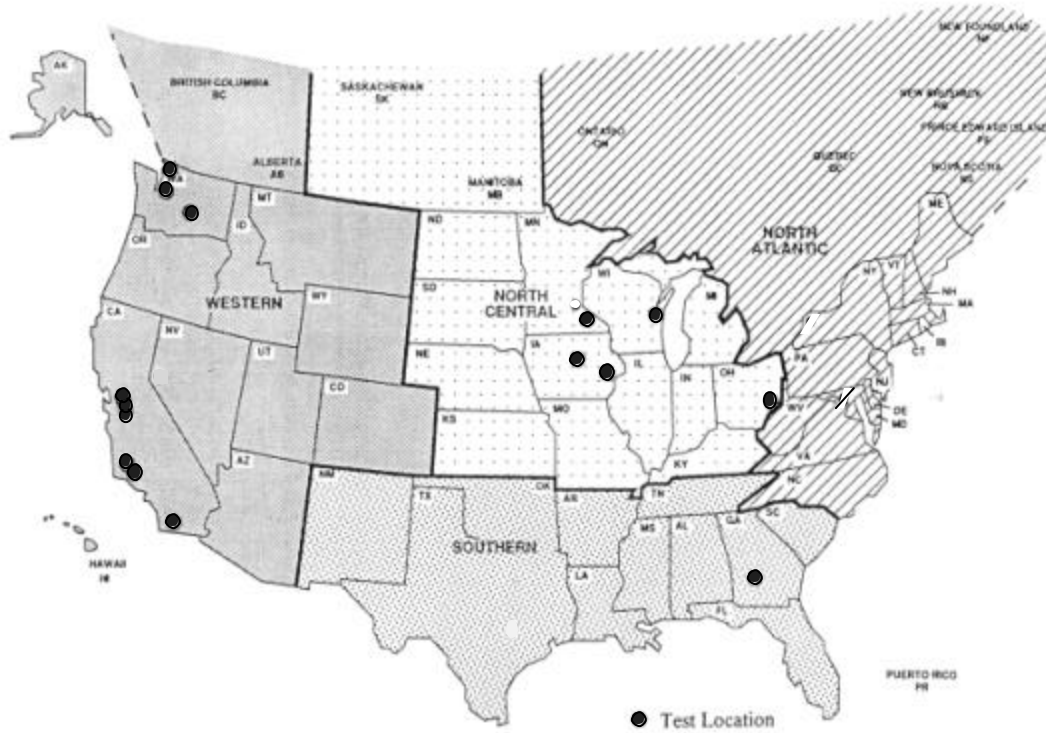


Figure 3.1.3 General locations of the 15 selected test sections. The shadings indicate the geographical region.

**Table 3.1.1** Pavement system information for the studied test sections determined from the LTPP database and field investigations.

Climate	State	Section	Const. Date	Age at Testing (Years)	Estimated Cum. ESAL's (Millions)	Joints			Layer Information				
						Type	Avg. Spacing (m)	Random Spacing (m)	Pavement Type	Base Type	Layer Thicknesses		
											PCC (mm)	Base (mm)	Subbase (mm)
DNF	06	3017	7/1/78	19.50	3.90	Agg	4.7	3.65, 3.96, 5.79, 5.49	JPCP	CTB	202	84	235
	06	3021	4/1/74	24.00	5.25	Agg	4.7	3.65, 5.50, 5.80, 3.95	JPCP	CTB	207	150	No Sub.
	06	7456	12/1/71	26.00	16.00	Agg	4.7	3.65, 5.50, 5.80, 3.95	JPCP	CTB	297	137	608
	06	CS1	12/1/71	26.00	16.00	Agg	4.7	3.65, 5.50, 5.80, 3.95	JPCP	CTB	224	137	608
	06	CS3	12/1/71	26.10	16.00	Agg	4.7	3.65, 5.50, 5.80, 3.95	JPCP	CTB	212	114	608
	06	I-10	1946	51.00	>16.00	Agg	4.7	3.65, 5.50, 5.80, 3.95	JPCP	CTB	224	106	235
DF	53	3019	8/1/86	11.20	6.21	Agg	3.5	2.74, 3.05, 4.27, 3.96	JPCP	CTB	252	127	229
WF	19	3006	11/1/75	21.80	3.97	Dow	6.1	--	JPCP	CTB	225	84	141
	19	3055	8/1/69	28.10	4.27	Agg	6.1	--	JPCP	Gravel-Uncrushed	250	84	No Sub.
	27	4054	10/1/72	24.90	10.70	Dow	8.2	--	JRCP	Crushed Stone	243	151	1016
	39	3801	1/1/84	13.40	4.69	Dow	6.1	--	JPCP	CTB	238	108	No Sub.
	55	3008	12/1/75	21.70	15.20	Agg	4.7	3.96, 5.79, 5.49, 3.65	JPCP	Crushed Gravel	277	152	No Sub.
WNF	53	3011	6/1/77	20.40	8.93	Agg	3.5	4.3, 4.0, 2.7, 3.0	JPCP	-	248	No Base	1016
	53	3812	3/1/65	32.60	12.77	Agg	4.6	--	JPCP	Coarse Soil Agg. Mix	224	165	No Sub.
	13	GA1-5/6	6/1/71	26.10	23.00	Dow	6.1	--	JPCP	CTB (GA1-5) ATB (GA1-6)	232	142	319

27-4054 has 1016 mm (40 in) embankment over loose/soft clayey silt

53-3011 has 1016 mm (40 in) embankment over glacial sandy gravelly clay/clayey sand and gravel

\* Estimated total traffic

**Table 3.1.2** Environmental data for the studied test sections, primarily from the LTPP database.

Climate	State	Section	Annual Precipitation (mm)	AVG Days Below 0 °C (32 °F)	AVG Days Above 32 °C ( 90 °F)	AVG Days Wet per Year	Days with 127 mm (0.5in) Precip. per Year	Yearly Freeze-Thaw Cycles	USCOE Freeze Index
DNF	06	3017	508	1	60	45	12	1	0
	06	3021	447	63	70	53	11	73	2
	06	7456	277	16	70	58	5	22	1
	06	CS1	277	16	70	58	5	22	1
	06	CS3	277	16	70	58	5	22	1
	06	I10	508	1	60	45	12	1	0
DF	53	3019	170	70	35	66	0	64	215
WF	19	3006	848	128	14	135	18	84	1037
	19	3055	828	148	12	117	20	91	1400
	27	4054	846	152	9	134	19	91	1546
	39	3801	1019	110	11	146	25	92	458
	55	3008	861	129	1	165	17	82	891
WNF	53	3011	912	53	0	140	17	54	98
	53	3812	950	19	2	141	21	22	29
	13	GA1-5/6	NA	NA	NA	NA	NA	NA	NA

Of the 15 pavement sections, 11 were chosen from the LTPP database because of the wealth of pavement data available for these sites. The other four pavements were selected outside the LTPP database for various reasons. One of these pavements, the I-10 section by Etiwanda, just east of Los Angeles, was selected based on information by Caltrans that it was constructed in 1946 and had performed well, though it consisted of regular strength concrete. The other three pavements were older JPCP's from experimental test roads in California and in Georgia. The California test road, on I-5 near Tracy, included two sections of interest to this study in addition to section 06-7456 from LTPP database. One was a control section with the same mix design as section 06-7456, but with a decreased slab thickness. The other was a test section of the same thickness as the control section, but with higher strength PCC. For these test sections the same aggregates were used in the mix.

The Georgia section, brought to the attention of the research team by FHWA, was an older JPCP of lower strength concrete. A major design difference was the use of doweled joints on the Georgia test road to control faulting. This pavement turned out to be important for this study as it shared several important characteristics with the control section on I-5 in Tracy, California. Both were without subsurface drainage, JPCP's on CTB's, of the same age (26 years), in mild climates (WNF versus DNF), of the same slab thickness, and subject to high traffic loading (23 million ESAL's versus 16 million for the California test road). The main differences between these two sections are performance related. The Georgia section has virtually no distress. This was even more significant when considering that it consisted of long 6.1-m (20-ft) PCC slabs, which is at the upper recommended limit for design of JPCP to avoid transverse slab cracking. In comparison, the longer of the I-5 JPCP slabs (> 3.96 m (13 ft)) on CTB in California developed low to medium severity transverse cracks over time, except when a much thicker slab design was used as for the 06-7456 section.

Of the studied pavement sections, four were older sections with high distress levels. They were selected in order to better evaluate whether the differences in key PCC properties result in either low or high distress levels in terms of joint/crack faulting, spalling and transverse cracking. Two of these four sections from the WF climate zone were of particular interest. The Wisconsin section 55-3008, was found to have an in-place compressive strength of 62 MPa (9000 lbf/in<sup>2</sup>) with the highest level of faulting in the LTPP database. It is undoweled with high cumulative ESAL's. The Iowa section 19-3006, was selected because it had the highest level of spalling according to LTPP. The in-place strength was 56 MPa (8100 lbf/in<sup>2</sup>). Both these sections were older pavements of similar age (21.7-21.8 years) at time of testing.

Three high strength concrete pavements with excellent performance were selected from Washington State. These pavements had in-place compressive strengths up to 75 MPa (10,900 lbf/in<sup>2</sup>), and contained durable aggregates. At section 53-3812 located near Seattle, WA, on I-5, the pavement was over 30 years old. A previous study had attributed the unusually good performance to combinations of good foundation design, mild environmental conditions, high quality aggregates in the concrete mix, and higher than normal strength. (Mahoney et al., 1991).

**3.1.1 Test Sections in the DNF and DF Regions**

**Test Section 06-3017**

Test section 06-3017 is located in California on State Route 2, Glendale. The field investigation was executed on December 10, 1997. The pavement was constructed in 1978 and was about 20 years old at the time of testing. The test section was placed on a tangent/elevated section on a plus grade (uphill) in the direction of traffic, and it is located on a deep fill greater than 12.2 m (40 ft). The pavement section consisted of about 185- to 215-mm (7.25- to 8.5-in) plain concrete on an 85-mm (3.3-in) cement aggregate mixture, and a 150-mm (6-in) coarse soil aggregate mixture subbase. The subgrade consisted of silty sand and gravel. It is possible this was embankment/fill material. Coring showed that there was no bond between the concrete and the base layers. The DCP indicated excellent support conditions. There was no evidence of a subsurface drainage system. The pavement transverse joints were skewed 60 cm (2 ft) per lane, and the load transfer was achieved by aggregate interlock. The joint spacing averaged 4.7 m (16 ft), but varied from 3.65, 5.50, 5.80, and 3.95 m (12, 18, 19, and 13 ft) and repeating. Both the inside and the outside shoulders were constructed with asphalt concrete.

The test section was in excellent condition with only a minor amount of faulting, which was on the order of 0.5 to 2 mm, with two joints having faulting of 5.7 mm. Three longitudinal joints exhibited medium severity of spalling with a total length of 0.8 m (31 in). The concrete surface showed map cracking, but it did not appear to have affected the concrete durability or the concrete surface condition.



*Figure 3.1.4 Overview of test site 06-3017.*



*Figure 3.1.5 Distress free slab and joint in test site 06-3017.*

**Test Section 06-3021**

Test section 06-3021 was located in California on I-8, Buckman Springs. The field investigation was executed on December 11, 1997. The pavement was constructed in 1974 and was about 24 years old at the time of testing. The test section was placed on a tangent/elevated section on a plus grade (very shallow uphill) in the direction of traffic, and it was located on a cut of about 1.8 to 4.6 m (6 to 15 ft). The pavement section consisted of about 200- to 215-mm (8- to 8.5-in) plain concrete on a 135- to 165-mm (5.25- to 6.5-in) CTB, and coarse grained subgrade of micaceous sand with trace-to-some silt. Coring showed that there was no bond between the concrete and the base layers. The DCP indicated good support conditions. There was no evidence of a subsurface drainage system. The pavement transverse joints were skewed 60 cm (2 ft) per lane, and the load transfer was achieved by aggregate interlock. The joint spacing varied from 3.65, 5.50, 5.80, and 3.95 m (12, 18, 19, and 13 ft) and repeating. Both the inside and the outside shoulders were constructed with asphalt concrete.

The test section was in good condition and had undergone some maintenance work (patching). The test section had only a minor amount of faulting that was on the order of 1 to 3 mm, with the largest faulting of 4.5 mm. About 75 percent of the transverse joints suffered from low severity spalling, and some spalling was observed for longitudinal joints. The concrete surface showed map cracking, but it did not appear to have affected the concrete durability or the concrete surface condition.



*Figure 3.1.6 Overview of test site 06-3021.*



*Figure 3.1.7 Distress free slab at test site 06-3021.*



**Tracy Test Road Sections (06-7456, 06-CS1, and 06-CS3)**

Three pavement sections were tested from the Tracy Test Road, located in California, near Tracy. These included the SHRP section 06-7456, and two control sections (CS), labeled in this report as sections 06-CS1 and 06-CS3. Sections 06-7456 and 06-CS1 are identical from a concrete materials perspective, though 06-7456 has a thicker concrete section of 30 cm (12 in) compared to 22 cm (8.8 in) for section 06-CS1. Section 06-CS3 has the same pavement cross section design as 06-CS1, but has a mix design with a higher cement content.

**Test Section 06-7456 (Tracy Test Road)**

Test section 06-7456 is the SHRP LTPP test section from the Tracy Test Road. The pavement was constructed in 1971 and was about 26 years old at the time of testing. The test section was placed on a tangent on a plus grade (very shallow uphill) in the direction of traffic, and it was located in a fill with an estimated thickness of 1.5 m (5 ft). The pavement section consisted of about 300-mm (12-in) plain concrete on a 135- to 140-mm (5.25- to 5.5-in) CTB, and coarse grained subbase of sandy gravel. The natural subgrade was not encountered during sampling. Coring showed that there was no bond between the concrete and the base layers. The DCP indicated very good support conditions. There was no evidence of a subsurface drainage system. The pavement transverse joints were skewed 60 cm (2 ft) per lane, and the load transfer was achieved by aggregate interlock. The joint spacing varied from 3.65, 5.50, 5.80, and 3.95 m (12, 18, 19, and 13 ft) and repeating. Both the inside and the outside shoulders were constructed with asphalt concrete.

The test section was in excellent condition. The test section had only a minor amount of faulting, on the order of 0 to 4 mm.



*Figure 3.1.8 Overview of test site 06-7456, Tracy Test Road.*



*Figure 3.1.9 No slab distress at test site 06-7456, Tracy Test Road.*

***Test Section 06-CS1 (Tracy Test Road)***

Test section 06-CS1 is the control section of the Tracy Test Road. The field investigation was executed on December 31, 1997. The pavement was constructed in 1971 and was about 26 years old at the time of testing. The test section was placed on a tangent on a plus grade (very shallow uphill) in the direction of traffic, and it was located in a fill with an estimated thickness of 1.5 m (5 ft). The pavement section consisted of about 225- to 230-mm (8.75- to 9-in) plain concrete on a 135- to 140-mm (5.25- to 5.5-in) CTB, and coarse grained subbase of sandy gravel. The natural subgrade was not encountered during sampling. Coring showed that there was no bond between the concrete and the base layers. The DCP indicated very good support conditions. There was no evidence of a subsurface drainage system. The pavement transverse joints were skewed 60 cm (2 ft) per lane, and the load transfer was achieved by aggregate interlock. The joint spacing varied from 3.65, 5.50, 5.80, and 3.95 m (12, 18, 19, and 13 ft) and repeating. Both the inside and the outside shoulders were constructed with asphalt concrete.

The test section was in fair condition. On the longer slabs, low and medium severity corner breaks and transverse cracks were observed. The shorter slabs were found in very good condition. The test section had only a minor amount of faulting, on the order of 0 to 5 mm. Residue left from pumping of fines at the pavement edge adjacent to many transverse joints was observed. The pumping evidence was also observed at some transverse cracks. The concrete surface showed map cracking, but it did not appear to have affected the concrete durability or the concrete surface condition.



***Figure 3.1.10*** Medium severity transverse crack at 06-CS1, Tracy Test Road (control section).



***Figure 3.1.11*** Corner break near approach joint at 06-CS1, Tracy Test Road (control section).

***Test Section 06-CS3 (Tracy Test Road)***

Test section 06-CS3 is section 3 of the Tracy Test Road. The field investigation was executed on December 4, 1997. The pavement was constructed in 1971 and was about 26 years old at the time of testing. The test section was placed on a tangent on a plus grade (very shallow uphill) in the direction of traffic, and it was located on a fill with an estimated thickness of 1.1 m (3.5 ft). The pavement section consisted of about 210- to 215- mm (8.25- to 8.5- in) plain concrete on a 75- to 130-mm (3- to 5-in) CTB, and coarse grained subbase of sandy gravel. The natural subgrade was not encountered during sampling. Coring showed that there was no bond between the concrete and the base layers. The DCP indicated very good support conditions. There was no evidence of a subsurface drainage system. The pavement transverse joints were skewed 60 cm (2 ft) per lane, and the load transfer was achieved by aggregate interlock. The joint spacing varied from 3.65, 5.50, 5.80, and 3.95 m (12, 18, 19, and 13 ft) and repeating. Both the inside and the outside shoulders were constructed with asphalt concrete.

The test section was in fair condition. Low to medium severity transverse cracks were observed on 2/3 of the slabs, with only the 3.65-m (12-ft) slabs unaffected. There were two locations with low severity corner breaks. The test section had only a minor amount of faulting, on the order of 0 to 6 mm, with an average of 2 to 3 mm. Residue left from pumping of fines at the pavement edge adjacent to many transverse joints was observed. The concrete surface, the wheel path in particular, showed map cracking, but it did not appear to have affected the concrete durability or the concrete surface condition. This test section, 06-CS3, exhibited twice the number of transverse cracks as compared to the control section, 06-CS1, and also the amount of faulting was higher for this section. However, the spalling of this section was only half of that observed at the control section.



***Figure 3.1.12*** Crack only in truck lane at 06-CS3, Tracy Test Road (control section).



***Figure 3.1.13*** Corner break in truck lane at 06-CS3, Tracy Test Road (control section).

**Test Section 06-I-10**

Test section 06-I-10 was located in California on I-10, Etiwande, at the Ontario site. The field investigation was executed on December 9, 1997. The pavement was constructed in 1946 and was about 51 years old at the time of testing. The test section was placed on a tangent on a minus grade (very shallow downhill) in the direction of traffic, and it was located in a cut/fill transition. The pavement section consisted of about 215- to 235- mm (8.5- to 9.25-in) plain concrete on a 75- to 120- mm (3- to 4.75-in) CTB, and coarse grained subbase of sandy gravel. The natural subgrade was not encountered during sampling. Coring showed that there was no bond between the concrete and the base layers. The DCP indicated very good support conditions. There was no evidence of a subsurface drainage system. The pavement transverse joints were skewed 60 cm (2 ft) per lane, and the load transfer was achieved by aggregate interlock. The joint spacing varied from 3.65, 5.50, 5.80, and 3.95 m (12, 18, 19, and 13 ft) and repeating. Both the inside and the outside shoulders were constructed with asphalt concrete.

The test section was in good condition. Low to medium severity transverse cracks were observed on 25 percent of the slabs, and tended to occur on the 5.5- and 5.8-m (18- and 19- ft) slabs. About 2/3 of the transverse joints were observed to have low severity of spalling, and most of the joints had minor severity faulting averaging about 2 to 3 mm.



*Figure 3.1.14 Overview of test site 06-I-10.*



*Figure 3.1.15 Transverse crack at test site 06-I-10 closer to leave joint.*

**Test Section 53-3019**

Test section 53-3019 was located in Washington on I-82, Benton County. The field investigation was executed on October 6, 1997. The pavement was constructed in 1986 and was about 11 years old at the time of testing. The test section was placed on a tangent section on a plus grade (uphill) in the direction of traffic, and it was located in a fill section with a fill thickness exceeding 12.2 m (40 ft). The pavement section consisted of about 250-mm (9.9-in) plain concrete on a 130-mm (5-in) crushed gravel base, and 90 mm (3.5 in) of silty sand with some gravel subbase. The subgrade consisted of silt with some fine sand. The DCP indicated excellent support conditions. There was no evidence of a subsurface drainage system. The pavement transverse joints were skewed 60 cm (2 ft) per lane, and the load transfer was achieved by aggregate interlock. The joint spacing was 4.3, 4.0, 2.7, and 3.0 m (14, 13, 9, and 10 ft) and repeating. Both the inside and the outside shoulders were constructed with asphalt concrete.

This pavement section was in excellent condition. There was abrasion of the pavement surface in the wheel paths, likely caused by use of tire chains and/or studded tires. The finer aggregate and paste had eroded projecting the coarse aggregate above the surrounding pavement surface. There had been no maintenance activities on the test section. Most transverse joints exhibited low severity spalling, and an isolated longitudinal joint suffered from spalling. Transverse joint faulting ranged from 0 to 1.6 mm.



*Figure 3.1.16 Overview of test site 53-3019.*



*Figure 3.1.17 Typical distress free slab at 53-3019.*

**3.1.2 Test Sections in the Wet Freeze Region**

**Test Section 19-3006**

Test section 19-3006 was located in Iowa on US-30, in Clinton County. The field investigation was executed on August 27, 1997. The pavement was constructed in 1975 and was about 22 years old at the time of testing. The test section was placed on a tangent section on a plus grade (uphill) in the direction of traffic, and it was located in a fill section with a fill depth estimated to be between 0.6 to 0.9 m (2 and 3 ft). The pavement section consisted of about 230-mm (9-in) plain concrete on a 115-mm (4.5-in) CTB on about 150 mm (6 in) of silty sand subbase. The subgrade was sandy and silty clays. There was only a slight bonding between the PCC and the base. The DCP indicated poor to marginal support conditions. There was no evidence of a subsurface drainage system. The pavement transverse joints were normal, and the load transfer was achieved through 31.75-mm (1.25-in) dowel bars. The joint spacing was on average 6.1 m (20 ft). Both the inside and the outside shoulders were constructed with a gravel surfacing.

The test section was in very poor condition with all joints exhibiting some degree of spalling. High and low severity spalling with loss of material was noted at 22 of the 26 joints. Transverse joint faulting ranged from about 0.2 to 8.5 mm, with an average of about 3 mm. Previous survey records indicate that this section has been deteriorating rapidly since 1994.



*Figure 3.1.18 Typical transverse joint distress at 19-3006.*



*Figure 3.1.19 Close-up on transverse joint spalling at 19-3006.*

**Test Section 19-3055**

Test section 19-3055 was located in Iowa on US-20, in Hamilton County. The field investigation was executed on August 28, 1997. The pavement was constructed in 1968 and was about 29 years old at the time of testing. The test section was placed on a tangent section on a minus grade (downhill) in the direction of traffic, and it was located in a fill section with a fill depth estimated to be between 0.6 to 0.9 m (2 to 3 ft). The pavement section consisted of about 250-mm (10-in) plain concrete on a 75-mm (3-in) dense graded aggregate base on sandy clay subgrade. The DCP indicated marginal to poor support conditions. The pavement transverse joints were normal, and the load transfer was achieved by aggregate interlock. The joint spacing was on average 6.1 m (20 ft). Both the inside and the outside shoulders were constructed with an asphalt concrete surface.

The test section was in very good condition with only low severity spalling of the transverse joints and transverse joint faulting ranging from 0 to 6.6 mm with an average of 3 mm. Some of the light spalling may have been due to snow plowing.



*Figure 3.1.20 Typical distress free slab at 19-3055.*



*Figure 3.1.21 Transverse joint in good condition at 19-3055.*

**Test Section 27-4054**

Test section 27-4054 was located in Minnesota on I-90, Winona County. The field investigation was executed on August 26, 1997. The pavement was constructed in 1972 and was about 25 years old at the time of testing. The test section was placed in a transition between an elevated and a tangent section on a plus grade (uphill) in the direction of traffic, and it was located in a cut section with a cut depth between 1.8 and 4.6 m (6 and 15 ft). The pavement section consisted of about 240-mm (9.5-in) wire mesh reinforced concrete on a 150-mm (6-in) crushed stone base on a sand subbase. This sand was not believed to be the subgrade. The DCP indicated excellent support conditions. There was no evidence of a subsurface drainage system. The pavement transverse joints were skewed 60 cm (2 ft) per lane, and the load transfer was achieved by 25-mm (0.975-in) round dowel bars. The joint spacing averaged 8.2 m (27 ft). Both the inside and the outside shoulders were constructed with asphalt concrete.

The test section was in a relatively good condition except for the faulting, which ranged from 0.8 to 7.5 mm, two small high severity corner breaks, and low severity transverse joint spalling due in part to snow plowing.



*Figure 3.1.22 Overview of test site 27-4054.*



*Figure 3.1.23 Corner break and repair at 27-4054.*



**Test Section 39-3801**

Test section 39-3801 was located in Ohio on SR-7 in Belmont County. The field investigation was executed on June 5, 1997. The pavement was constructed in 1984 and was about 13 years old at the time of testing. The pavement section consisted of about 210- to 245- mm (8.25- to 9.65-in) plain concrete on a 120- mm (4.65- in) cement-aggregate mixture base, and a subgrade consisting of silty clay with some gravel and trace of sand. The DCP indicated good to excellent support conditions. There was no evidence of a subsurface drainage system. The pavement transverse joints were normal, and the load transfer was achieved by 24.8- mm (0.975- in) round dowel bars. The joint spacing averaged 6.1 m (20 ft). Both the inside and the outside shoulders were constructed with asphalt concrete.

The test section was in good condition. All transverse joints exhibited low severity of spalling, and faulting which ranged from -1.3 to 0.7 mm. Furthermore, a significant amount of low severity longitudinal cracking was observed at dowel bars.



*Figure 3.1.24 Overview of test site 39-3801.*



*Figure 3.1.25 Close-up of distress free transverse joint at 39-3801.*

**Test Section 55-3008**

Test section 55-3008 is located in Wisconsin on I-43, in Ozaukee County. The field investigation was executed on July 29, 1997. The pavement was constructed in 1975 and was about 22 years old at the time of testing. The test section was placed on a tangent section on a plus grade (uphill) in the direction of traffic, and it was located in a cut section with a cut depth estimated to be between 1.8 and 4.5 m (6 and 15 ft). The pavement section consisted of about 265- to 280-mm (10.4- to 11-in) plain concrete. The pavement foundation consisted of a 150-mm (6-in) crushed gravel subbase on a silty clay subgrade. The DCP indicated marginal to good support conditions. There was no evidence of a subsurface drainage system. The pavement transverse joints were skewed 60 cm (2 ft) per lane, and the load transfer was achieved by aggregate interlock. The joint spacing was on average 4.7 m (16 ft) but varied from 3.70 to 5.50 m. Both the inside and the outside shoulders were constructed with asphalt concrete that recently had been surface treated.

The test section was in good condition except for faulting, which ranged from 4.3 to 15.2 mm, and low severity of transverse cracking. In addition the outside lane was faulted 3 to 6 mm relative to the inside lane. One medium severity crack was observed. There was no evidence of pumping of the subgrade, nor had any maintenance been required (except diamond grinding before and after the test section).



*Figure 3.1.26 Overview of test site 55-3008.*



*Figure 3.1.27 Transverse joint at 55-3008 (faulting of shoulder).*

**3.1.3 Test Sections in the Wet No Freeze Region**

**Test Section 53-3011**

Test section 53-3011 was located in Washington on I-5, Whatcom County. The field investigation was executed on October 2, 1997. The pavement was constructed in 1977 and was about 20 years old at the time of testing. The test section was placed on a tangent section on a plus grade (uphill) in the direction of traffic, and it was located in a cut section with a cut depth estimated to be between 1.5 and 4.5 m (5 and 15 ft). The pavement section consisted of about 250-mm (9.75-in) plain concrete on a 355- to 380-mm (14- to 15-in) subbase that consisted of coarse-grained soil-aggregate mixture (SAM). The subgrade was silty sand. The DCP indicated excellent support conditions. There was no evidence of a subsurface drainage system. The pavement transverse joints were skewed 60 cm (2 ft) per lane, and the load transfer was achieved by aggregate interlock. The joint spacing was 4.3, 4.0, 2.7, and 3.0 m (14, 13, 9, and 10 ft) and repeating. Both the inside and the outside shoulders were constructed with asphalt concrete.

The test section was in very good condition, and there were no maintenance activities on the test section. Most transverse joints exhibited low severity spalling, and a few isolated longitudinal joints suffered from spalling. The transverse joint faulting ranged from 0 to 5 mm. There was abrasion of the pavement surface in the wheel paths, likely caused by use of tire chains and/or studded tires. The finer aggregate and paste had eroded, projecting the coarse aggregate above the surrounding pavement surface.



*Figure 3.1.28 Overview of test site 53-3011 (above).*



*Figure 3.1.29 Joint core sample in good condition from section 53-3011 (right).*

**Test Section 53-3812**

Test section 53-3812 was located in Washington on I-5, Snohomish County. The field investigation was executed on September 30 - October 1, 1997. The pavement was constructed in 1964 and was about 33 years old at the time of testing. The test section was placed on an elevated section to the left on a minus grade (downhill) in the direction of traffic, and it was located in a cut section with a cut depth estimated to be between 1.8 and 4.5 m (6 and 15 ft). The pavement section consisted of about 230-mm (9-in) plain concrete on a 150- to 180-mm (6- to 7-in) dense graded aggregate base (DGAB). The subgrade was silty sand with gravel and frequent cobbles. The DCP indicated excellent support conditions. There was no evidence of a subsurface drainage system. The pavement transverse joints were normal, and the load transfer was achieved by aggregate interlock. The joint spacing was 4.6 m (15 ft). Both the inside and the outside shoulders were constructed with asphalt concrete.

This pavement section was in excellent condition. There was abrasion of the pavement surface in the wheel paths, likely caused by use of tire chains and/or studded tires. The finer aggregate and paste had eroded projecting the coarse aggregate (many particles exceeding 25 mm) above the surrounding pavement surface. No maintenance activities had been performed on the test section. Most transverse joints exhibited low severity spalling, and three isolated longitudinal joints suffered from spalling. The transverse joint faulting ranged from -3.0 to 2.5 mm. The faulting appeared to be related to the abrasion of the concrete surface and may not represent true faulting.



*Figure 3.1.30 Overview of test site 53-3812.*



*Figure 3.1.31 Close-up of a distress free transverse joint at 53-3812.*

### **Test Section 13-GA1-5 and 13-GA1-6**

Test sections 13-GA1-5 and 6 were located in Georgia near Newman. The field investigation was executed on July 15, 1997. The pavements were constructed in 1971 and were about 28 years old at the time of testing. The test sections were placed on a tangent section on a minus grade (downhill) in the direction of traffic, and were located in a cut section with a cut depth between 1.8 and 4.5 m (6 and 15 ft). Section 13-GA1-5 consisted of about 230-mm (9-in) jointed plain concrete on a 150-mm (6-in) CTB on about 300 mm (12 in) of sandy gravel subbase. Section 13-GA1-6 consisted of about 230-mm (9-in) jointed plain concrete on a 125-mm (5-in) asphalt treated base on about 350 mm (14 in) of sand subbase. The subgrade for both sections consisted of layered sandy clays and silty sands. The DCP indicated poor to very poor support conditions. There was no evidence of a subsurface drainage system.

The pavement transverse joints were skewed 60 cm (2 ft) per lane, and the load transfer was achieved by 30-mm (1.25-in) round dowel bars. The joint spacing was 6.1 m (20 ft). Both the inside and the outside shoulders were constructed with asphalt concrete.

These pavements were in excellent condition, with negligible faulting which was typically less than 1 mm. Section 13-GA1-6 exhibited very minor transverse joint spalling.



*Figure 3.1.32 Overview of test site 13-GA1-5.*



*Figure 3.1.33 Distress free transverse joint at 13-GA1-5.*

### 3.2 PCC Sample Description and Petrographic Analysis

Petrographic analysis was performed at the University of Michigan, Michigan Department of Transportation, and Michigan Technological University. The overall petrographic analysis was obtained by characterization of lapped core specimens with the unaided eye and by using a low-power stereo microscope with 80X maximum magnification. The primary aim was to characterize the texture (homogeneity) of the concrete and to determine the aggregate types present in both the coarse ( $\geq 4$  mm) and fine fraction ( $< 4$  mm). The lapped core sections were also analyzed for physicochemical deterioration, such as carbonation depth, dissolution, alkali-silica reactions and cracks. Finally, the volume fraction of coarse and fine aggregates, the cement paste, and the hardened air-void content was determined by the linear traverse method (ASTM C-457) at MDOT.

Selected samples were characterized through microscopic analysis of petrographic thin-sections to evaluate the homogeneity of the cement paste and the extent to which microcracking and formation of secondary phases has occurred in the concrete. These results are explained in detail in appendix B. Figure 3.2.1 shows the typical procedure for cutting the concrete core into a) the lapped section; which is used for overall petrographic analysis and composition by the linear traverse analysis; and b) thin-sections from top, middle and bottom.

The petrographic analysis of each sample is summarized by climatic region in sections 3.2.1 to 3.2.3 hereafter.

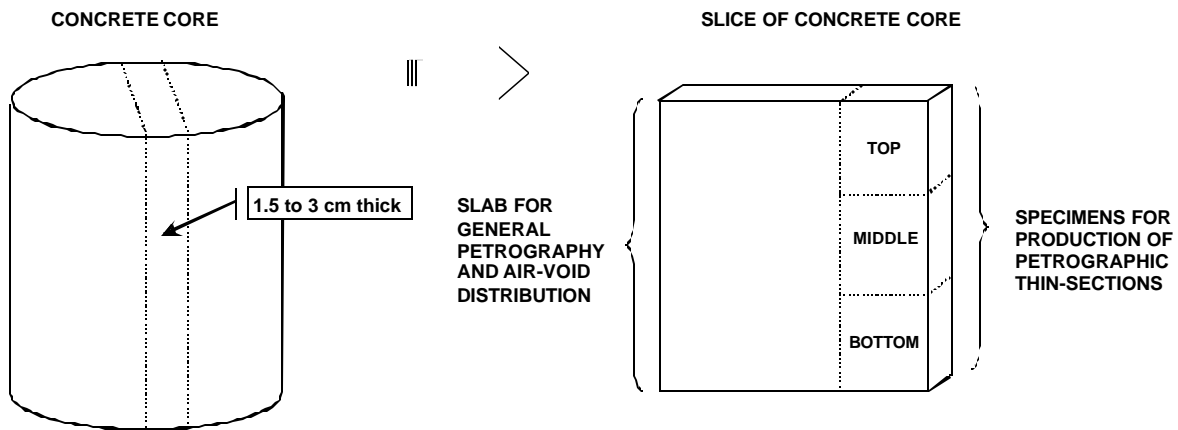


*Figure 3.2.1 Method for cutting the PCC drill-core into the lapped section and three thin-sections used for petrographic analysis.*

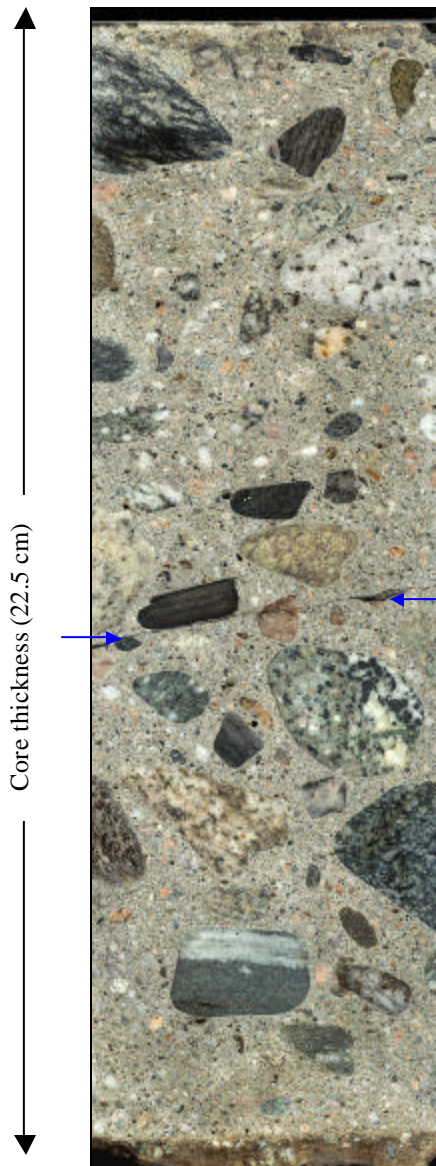
### 3.2.1 Petrographic Characterization of PCC Specimens from the Dry-No-Freeze and Dry-Freeze Regions

The specimens from the DNF region include the sections 06-3017, 06-3021, 06-7456, 06-CS1, 06-CS3, and 06-I-10 from California. Section 53-3019, from Washington, is in the DF region. All samples from the dry regions generally appear very well preserved. In two samples (06-3017 and 53-3019), the cement paste had been subjected to partial dissolution at the base of the pavement cores. Two samples (06-CS1 and 06-I-10) had been saw-cut and deterioration analysis at the top and base was not possible.

**Section ID: 06-3017**  
**State: California**  
**Climate: DNF**

*Table 3.2.1 Mix composition of 06-3017 by linear traverse (ASTM C457).*

Coarse Aggregate	Fine Aggregate	Paste Content	Air Content
49.3 vol.%	29.3 vol.%	14.0 vol.%	7.4 vol.%



The core-sample is 22.5 cm long and consists of rounded gravel in a medium gray cement paste (figure 3.2.2). The gravel consists of various silicate rocks (gabbro, quartz-rich rock fragments, biotite-rich gneiss and other metamorphic rocks). The largest aggregates are 46 mm (1.8 in). The packing of the coarse aggregate appears relatively open.

The fine aggregates mainly consist of angular to rounded quartz and quartz-rich rock-fragments, as well as biotite flakes. The carbonation depth was not determined.

The air voids are well-distributed in the concrete paste. A few large voids ( $\leq 17$  mm) of trapped air were also observed and typically occurred in connection with the larger aggregates. Locally, a red phase also occurred in these aggregates. Several air voids contain minor amounts of white crystallite precipitates.

The lower 1 to 2 cm of the concrete core is partially dissolved and impregnated with Fe-oxyhydrates. The alteration has left the base fragile and with coarse aggregates partially detached from the concrete paste.

Macro-cracks were not observed in the specimen. The crack observed in the image occurred during shipping of the sample (arrows).

**Figure 3.2.2** Polished cross-section of pavement section 06-3017.

**Section ID: 06-3021**

**State: California**

**Climate: DNF**

*Table 3.2.2 Mix composition of 06-3021 by linear traverse (ASTM C457).*

Coarse Aggregate	Fine Aggregate	Paste Content	Air Content
28.4 vol.%	43.4 vol.%	25.1 vol.%	3.1 vol.%

The core sample of 06-3021 is 20.5 cm long and consists of angular to rounded gravel in a medium gray cement paste (figure 3.2.3). The packing of the coarse aggregates appears relatively open. The cement paste in the top 15 mm is tanned and did not react with phenolphthalein indicating a deep carbonation depth.

The coarse aggregates ( $\leq 46$  mm) mainly consist of mafic to ultramafic igneous rocks. Minor amounts of coarse quartz and sandstone aggregates were also observed. The mafic aggregates readily rust after lapping indicating a high content of Fe- and/or Fe-Ti-oxides. The coarse aggregates are sometimes partially detached from the paste.

The fine aggregates mainly consist of angular to rounded quartz sand ( $\leq 2$  mm), as well as platy and fibrous aggregates of the mafic and ultramafic rocks observed in the coarse fraction. The fine aggregates are well-distributed in the paste.

The air voids are homogeneously distributed. However, large trapped air voids ( $\leq 17$  mm size) were abundant between 5.8 and 8.7 cm into the core. Several of the air voids contained white precipitates, but the specimen did not show indication of chemical alteration.

A few vertical cracks ( $\leq 11$  mm long) were observed close to the surface. A very fine ( $\ll 1$  mm) horizontal crack was observed at 7.5 cm below the surface. This crack is more than 2.5 cm long and runs from a 6-mm wide air void and propagates into the paste, deflecting around a coarse mafic aggregate and disappearing out of the specimen.

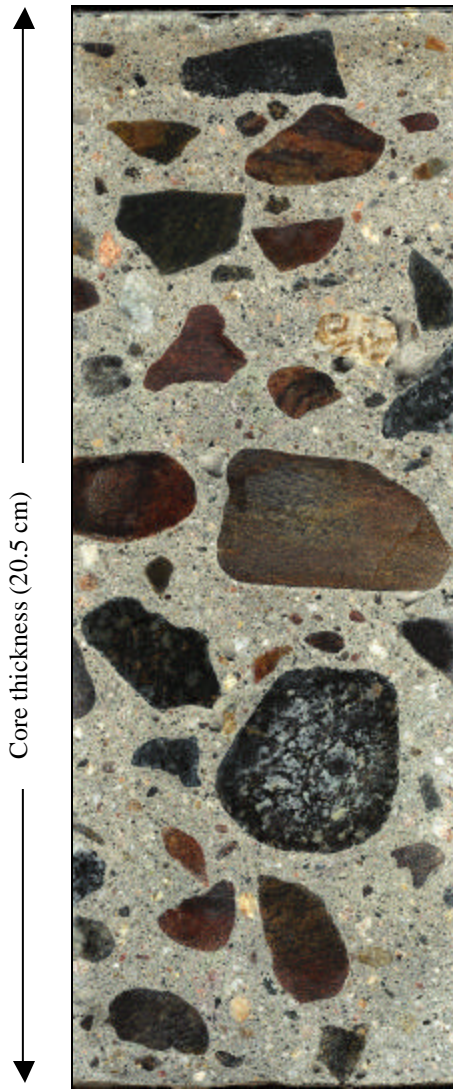


*Figure 3.2.3 Polished cross-section of pavement section 06-3021.*



**Section ID: 06-7456**  
**State: California**  
**Climate: DNF**

*Table 3.2.3 Mix composition of 06-7456 by linear traverse (ASTM C457).*

Coarse Aggregate	Fine Aggregate	Paste Content	Air Content
39.1 vol.%	31.1 vol.%	24.7 vol.%	5.1 vol.%

The core sample from section 06-7456 was 29.5 cm long and cut at the base. The concrete is composed of densely packed rounded to well-rounded gravel that is homogeneously distributed in a dark to medium gray cement paste. The carbonation depth was not determined.

The gravel consists of various rock types (gneiss, phyllosilicate-rich metasandstone, other metamorphic rock-types, and quartz-rich rock-fragments. A very thin reaction rim (< 0.5 mm) could be observed around some of the particles containing phyllosilicates as one of the constituent phases. The largest aggregate dimension observed was 7.5 mm, whereas the typical size of the largest aggregates was approximately 30 mm.

The fine aggregates mainly consist of rounded to sub-rounded sand with approximately equal amounts of quartz and rock fragments. The fine aggregates appear well distributed in the cement matrix.

The air voids are generally well distributed, but the total air-void content appears low. Larger air voids are present particularly in the upper 8 cm of the cores. The largest air void was 16 mm long and found in the middle of the section.

Fractures were observed in the upper half of the slab. The largest crack occurs at the very top of the slab and forms a closed loop deflecting at the surface at two larger aggregates at ~ 3.5 cm depth. The fracture may have formed due to cracking of finely layered dark-red siltstone and at detachment of a phyllosilicate-rich metasandstone particle at the very top of the slab. One aggregate of dark-brown shale, however, shows evidence of deleterious reaction with the paste that has resulted in concentric cracks within the aggregate and detachments at its surface. This particle was the only aggregate of this type observed in the slab.

**Section ID: 06-CS1**  
**State: California**  
**Climate: DNF**

*Table 3.2.4 Mix composition of 06-CS1 by linear traverse (ASTM C457).*

Coarse Aggregate	Fine Aggregate	Paste Content	Air Content
40.5 vol.%	24.6 vol.%	30.9 vol.%	4.0 vol.%

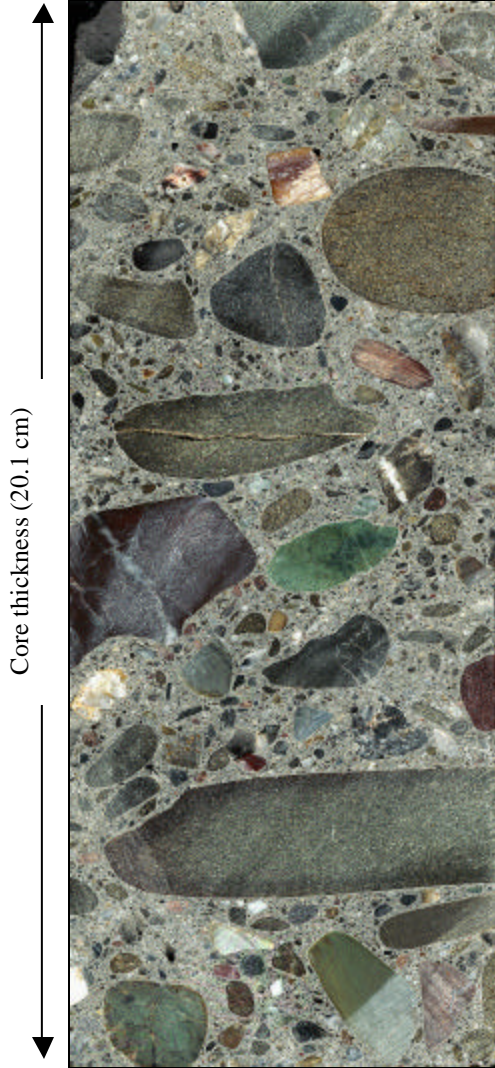


*Figure 3.2.4 Polished cross-section of pavement section 06-CS1.*

The core specimen was 20.1 cm long and cut at top and base. The concrete is composed by close-packed sub-rounded to well-rounded gravel in a dark to medium gray cement paste (figure 3.2.4).

The coarse aggregate mainly consists of fine to medium-grained metapelite, fine-grained gabbro, as well as green and red aggregates, likely to be siltstone. Some of the aggregates contain 1- to 2-mm size voids after dissolved sulfides. Single aggregates also contain up to 1-mm-wide internal cracks. The largest aggregates are more than 76 mm long and have an oblate shape (figure 3.2.4).

The fine aggregates consist of approximately 30 volume percent, quartz sand and 70 volume percent lithic fragments. Most of the fine aggregates appear rounded to sub-rounded and are well distributed in the paste.

The air voids are generally well dispersed. Several large air voids were, however, observed at the assumed base of the drill-core where a more than 15-mm sized air void was observed at the edge of the polished slab. The air voids occasionally contain white precipitates and botryoidal red aggregates.

A sub-horizontal fracture was observed between 7.5 and 9.5 cm into the sample. The crack had one end-point in a cracked aggregate but otherwise runs through the paste where it cuts some of the fine aggregates and deflects around the large aggregates. A small fracture was also observed at the top of the concrete in a sample analyzed at MDOT.

**Section ID: 06-CS3**

**State: California**

**Climate: DNF**

*Table 3.2.5 Mix composition of 06-CS3 by linear traverse (ASTM C457).*

Coarse Aggregate	Fine Aggregate	Paste Content	Air Content
30.7 vol.%	39.5 vol.%	25.5 vol.%	4.5 vol.%

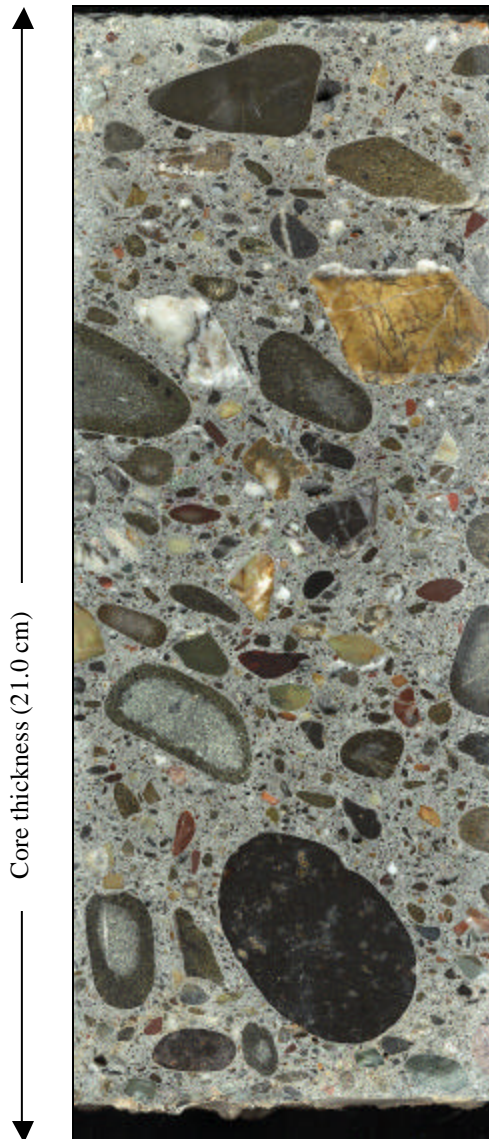


*Figure 3.2.5 Polished cross-section of pavement section 06-CS3.*

This concrete sample is 21 cm long and consists of rounded to well-rounded gravel dispersed in a dark, medium-gray cement paste (figure 3.2.5). Visually, there is tendency to an inhomogeneous distribution of the coarse aggregates ( $\leq 45$  mm). However, this may be caused by the relatively high abundance of larger aggregates. The coarse aggregates appear with a medium degree of packing. The carbonation depth was determined to be 1 to 2 mm.

The gravel consists of dolomitic limestone, sandstone, and siltstone, quartz, basalt, gabbro and metamorphic rocks. The dolomite aggregates contained 2 to 3-mm wide dark rims, probably related to weathering.

The fine aggregates mainly consist of angular to well-rounded quartz and lithic fragments of the same material as the coarse aggregates. Quartz is by far the most abundant aggregate type in the fraction below 1-mm size.

The air voids are well distributed and several air voids contain white precipitates which are inert in 0.1M HCl. Analysis of thin-sections has revealed that the precipitates mainly consist of ettringite. The white precipitates frequently fill the air voids below 9.5-cm depth in the core. Trapped air voids ( $\leq 14$  mm) are observed at all depths in the core.

A 2.1-cm long crack was observed on the surface of the drill-core but could not be traced in depth. At the base of the concrete core, drop-like precipitates had formed suggesting leaching and/or precipitation from trapped water in intergranular cavities below the concrete slab. Minor dissolution has occurred but is negligible.

**Section ID: 06-I-10**  
**State: California**  
**Climate: DNF**

*Table 3.2.6 Mix composition of 06-I-10 by linear traverse (ASTM C457).*

Coarse Aggregate	Fine Aggregate	Paste Content	Air Content
46.5 vol.%	25.7 vol.%	23.9 vol.%	3.9 vol.%

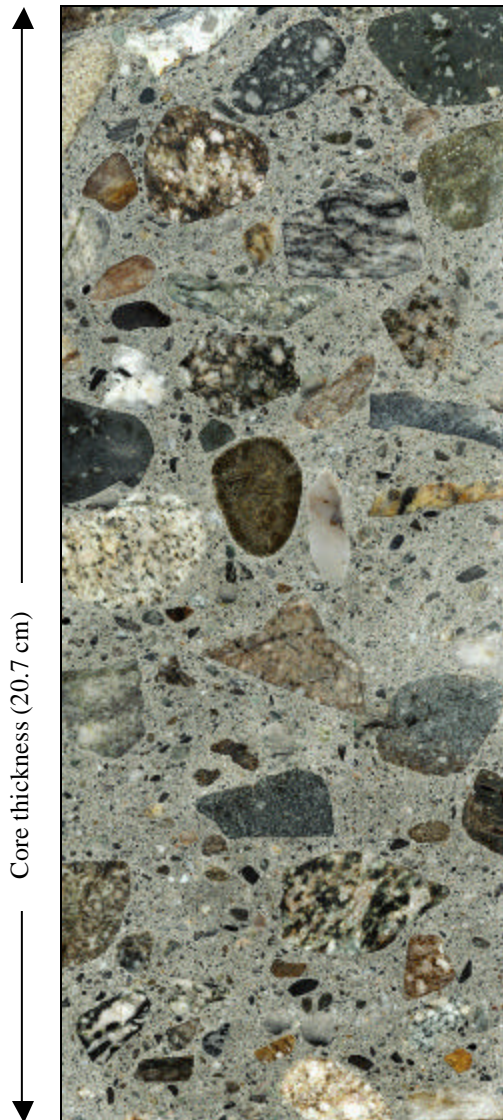


*Figure 3.2.6 Polished cross-section of pavement section 06 I-10.*

The polished slab from 06-I-10 was 20.7 cm long. The slab did not show the top and base of the drill-core and was not oriented. The concrete is composed by well-rounded gravel and a few angular rock fragments homogeneously dispersed with a relatively open packing in a medium gray concrete paste (figure 3.2.6).

The coarse aggregates consist of various gneiss-types, quartz, and minor amounts of porphyric basalt. The maximum size of the coarse aggregates was 44 mm in diameter. A few of the gneiss aggregates were partially altered.

The fine aggregates consist of angular to sub-rounded quartz sand with approximately 30 volume percent lithic fragments.

The number of air voids appears to be low. The largest air voids are 7 to 10 mm in diameter and mainly occur below 7 cm from the assumed top of the drill-core. Some of the air voids contain precipitates of a white phase.

**Section ID: 53-3019**  
**State: Washington**  
**Climate: DF**

*Table 3.2.7 Mix composition of 53-3019 by linear traverse (ASTM C457).*

Coarse Aggregate	Fine Aggregate	Paste Content	Air Content
45.9 vol.%	29.5 vol.%	15.5 vol.%	9.4 vol.%

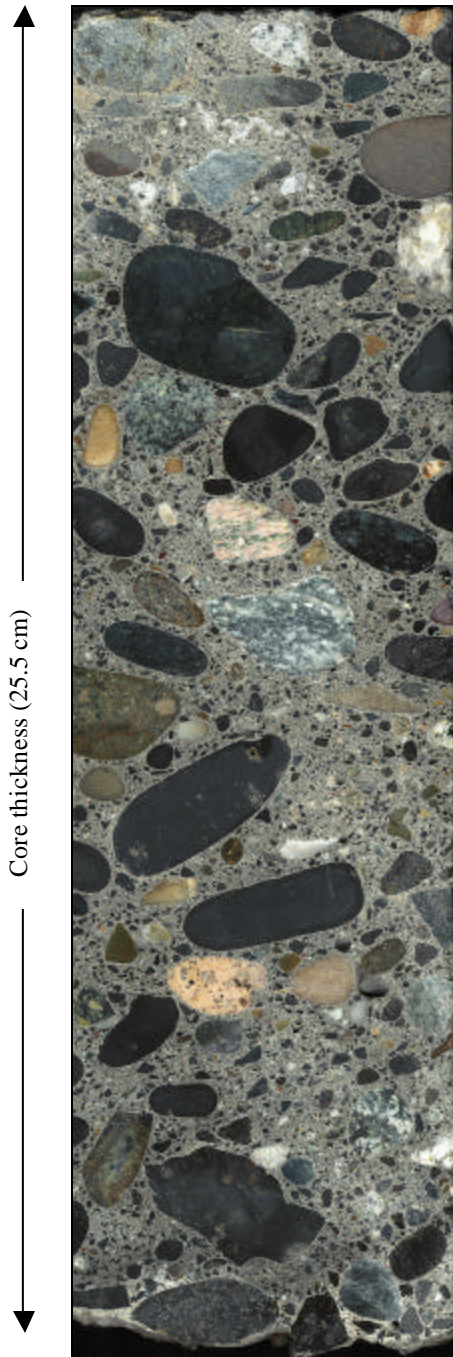


**Figure 3.2.7** Polished cross-section of pavement section 53-3019.

Sample 53-3019 is 25.5 cm long and mainly consists of up to 47-mm sized rounded to well-rounded aggregates of spherical to oblate shape dispersed in a dark gray cement paste (figure 3.2.7). The coarse aggregates show a medium degree of packing with slightly closer packing at the top 13.5 cm of the drill-core. The cement paste has a white coloration at the base of the concrete core and suggests that the paste has been subjected to minor dissolution (figure 3.2.7). The carbonation depth was not determined.

The coarse aggregates mainly consists of porphyric basalt (~ 75 volume percent) and minor amounts (~ 25 volume percent) of coarse-grained gabbro, granite, gneiss, and quartz (figure 3.2.7). A single angular aggregate of “recycled” concrete was also observed. Sometimes, the gneissic and granitic aggregates contained some porosity due to sulfide oxidation and secondary formation of Fe-oxhydrates. Most of the aggregates were surrounded by fine (<<1-mm-wide) white rims due to increased contents of fine air voids in at their interface. A few aggregates contained microcracks at their rims which resulted in the formation of local air-clusters and detachment of the aggregate from the cement paste.

The fine aggregates consist of angular to rounded quartz sand, as well as angular basalt and minor amounts of other lithic fragments that dominate in the 2 to 4-mm size fractions. The quartz sand strongly dominates in the fraction below 2-mm grain size.

The number of air voids appears to be high and they appear well-distributed in the paste. The largest air voids were 8.5 mm in diameter and located 9 cm below the surface. Most air voids were spherical but large angular pores of trapped air were also observed below 13.5-cm depth in the core.

### **3.2.2 Petrographic Characterization of PCC Sections from the Wet-Freeze Region**

The wet-freeze group consists of two samples from Iowa (19-3006 and 19-3055) and one sample from Minnesota (27-4054), one from Ohio (39-3801), and one from Wisconsin (55-3008). All concretes mainly contain coarse aggregates of carbonate-rocks. However, sample 39-3801 also contains important quantities of silicate rock aggregates. All the sections show dissolution of the paste and/or impregnation with secondary phases at their base. Moreover, paste alteration was prominent in 39-3801.

**Section ID: 19-3006**

**State: Iowa**

**Climate: WF**

**Table 3.2.8** Mix composition of 19-3006 by linear traverse (ASTM C457).

Coarse Aggregate	Fine Aggregate	Paste Content	Air Content
43.1 vol.%	29.2 vol.%	19.4 vol.%	8.3 vol.%

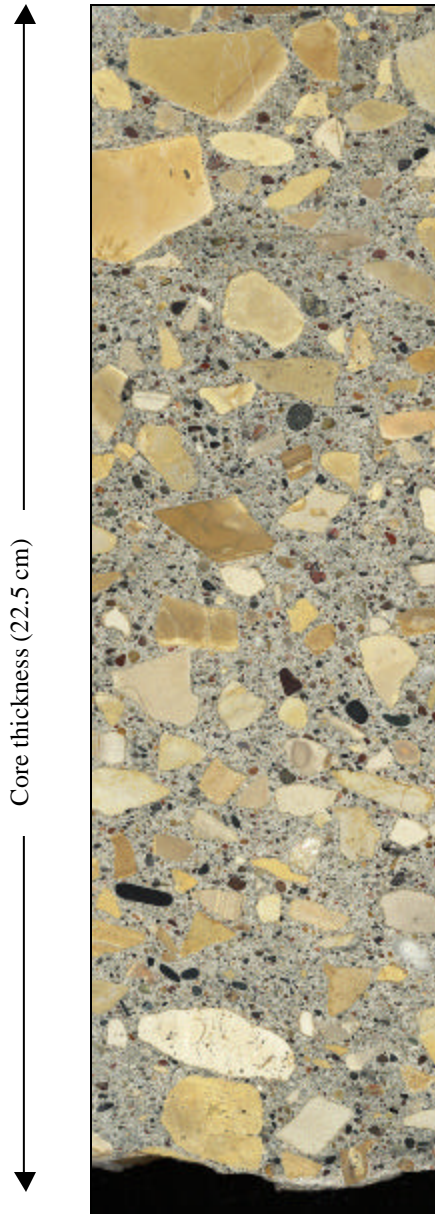


**Figure 3.2.8** Polished cross-section of pavement section 19-3006.

The drill-core of 19-3006 is 22.5 cm long. The concrete consists of angular and cream-white to beige-colored dolomite and a few fine-grained gabbroic rock-fragments dispersed in a medium gray cement paste (figure 3.2.8). The carbonation depth was 2 to 4 mm. The packing of the coarse aggregates was relatively open with a tendency to a closer packing in the upper 6 cm of the core.

The largest aggregate was 31 mm in diameter. The typical aggregate size was significantly smaller ( $\leq 15$  mm). Some dolomite aggregates have relatively large grain-sizes ( $\leq 0.25$  mm) and are often porous. Several of the beige-colored dolomite aggregates showed a white or weak reddish brown color zoning at the border to the paste. At these aggregates, the paste is typically white and shows increased porosity. The color change may be due to either de-dolomitization of the dolomite aggregate and/or oxidation of microscopical Fe-oxides in the dolomite. Similar observations were made by MTU.

The fine aggregates mainly consist of rounded to well-rounded sand with a typical grain-size below 2 mm. More than 60 volume percent of the sand consists of quartz. The rest of the sand-fraction consists of a wide variety of igneous and sedimentary rocks dominated by fine-grained mafic rocks.

The air voids are relatively small with a maximum size of 6 mm. The largest air voids are most abundant towards the base of the concrete core and typically occur in connection with the coarse aggregates.

A fine horizontal crack was observed at the base of the drill-core. The crack cuts both the paste and embedded aggregates in the concrete.

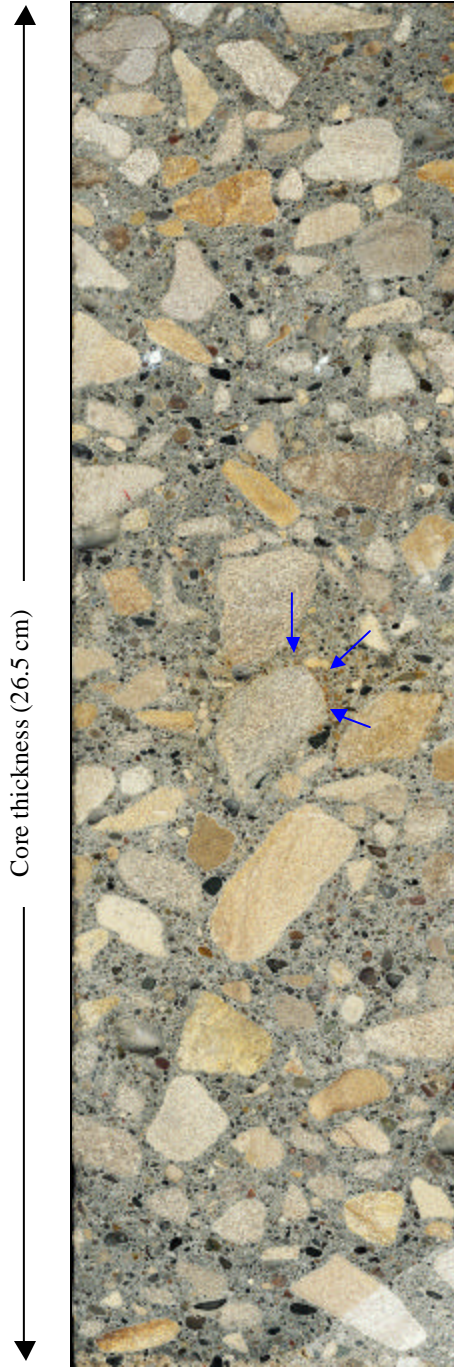
**Section ID: 19-3055**

**State: Iowa**

**Climate: WF**

**Table 3.2.9** Mix composition of 19-3055 by linear traverse (ASTM C457).

Coarse Aggregate	Fine Aggregate	Paste Content	Air Content
33.7 vol.%	28.0 vol.%	30.8 vol.%	7.5 vol.%



The drill-core of concrete 19-3055 is 26.5 cm long. The concrete is mainly composed by angular and sub-rounded gray and beige-colored dolomitic limestone embedded in a medium gray cement paste (figure 3.2.9). The coarse aggregates are evenly distributed and close packed. The carbonation depth is 2 to 3 mm.

The coarse aggregates consist of very fine-grained dolomite and more coarse-grained ( $\leq 1$  mm) oomicrite and/or pelmicrite. Minor gabbro aggregates are also present. Some of the coarse-grained dolomitic aggregates are porous and may show minor reaction with diluted HCl. The largest aggregates are up to 42-mm size in diameter. The typical aggregate size appears to be in the region of 15 to 20 mm. A rust-red coloration is locally observed in the paste around the some of the coarse aggregates (example shown at arrow in figure 3.2.9).

The fine aggregates consist of rounded to well-rounded quartz-rich sand and angular grains of dolomite, igneous, and metamorphic rocks. The grain size of the fine aggregates is typically below 2 mm. A few aggregates of dehydrated swelling clays were also observed. MTU identified some of the fine aggregates as the fragments of the “Pierre shale” which they claim is very reactive. MTU also observed minor but insignificant alkali-silica reactions at some of the fine aggregates.

The air voids are up to 11-mm size and generally homogeneously distributed in the paste. A few air voids contain white precipitates. Some of the precipitates were calcite. MTU reported that ettringite was abundant among the precipitates.

**Figure 3.2.9** Polished cross-section of pavement section 19-3055.



**Section ID: 27-4054**  
**State: Minnesota**  
**Climate: WF**

*Table 3.2.10 Mix composition of 27-4054 by linear traverse (ASTM C457).*

Coarse Aggregate	Fine Aggregate	Paste Content	Air Content
55.4 vol.%	17.9 vol.%	20.5 vol.%	6.2 vol.%

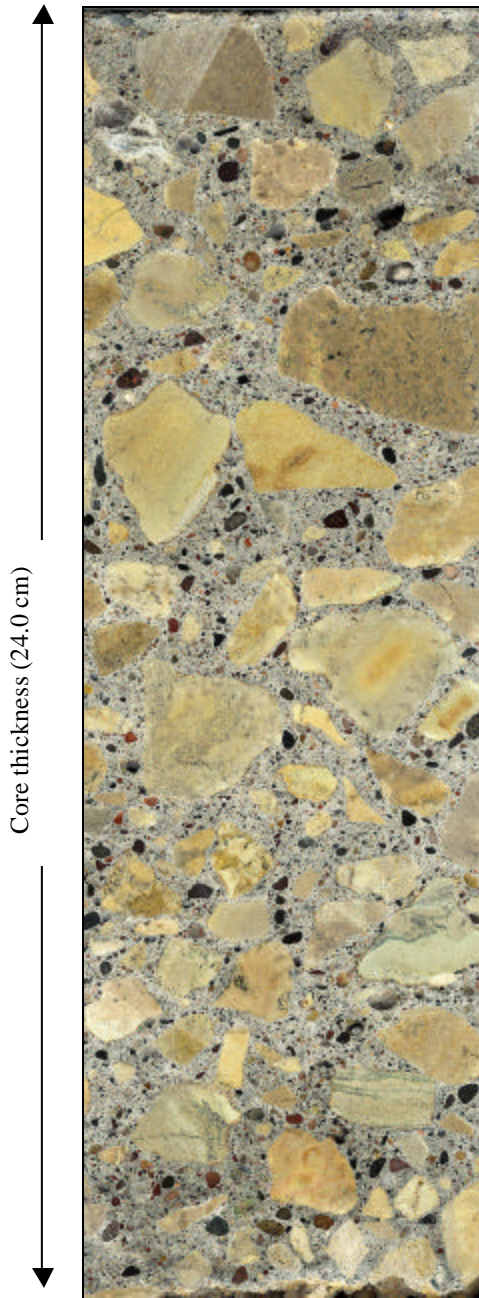


*Figure 3.2.10 Polished cross-section of pavement section 27-4054.*

The drill-core of pavement 27-4054 is 24.0 cm long and mainly consists of angular to sub-rounded dolomitic limestone in a light medium-gray cement paste (figure 3.2.10). Minor amounts of gabbro and other aggregate types are also present. The carbonation depth is 2 to 4 mm. The base of the concrete shows some sign of deterioration by partial dissolution of the cement paste and replacement with a yellow to red-brown brown phase(s).

The coarse aggregates are homogeneously distributed and appear to be relatively closely packed. The slab specimen showed the presence of more coarse aggregates at the top of the pavement section. This was, however, not confirmed by analysis of other sections from this site. The largest aggregate was more than 40 mm in diameter while the typical aggregate size appears to be 20 to 30 mm. Most of the coarse aggregates are porous, probably due to the volume reduction which occurs during dolomitization of calcite. Some of the coarse aggregates are rimmed by a 1- to 2-mm-wide reddish or white reaction rim.

The fine aggregates consist of sub-rounded to well-rounded quartz-rich sand with approximately 20 volume percent lithic fragments dominated by mafic rocks. Single nodules of swelling clays, up to 1 mm in size, were also observed in the paste. MTU observed reactive chert with idiomorphic carbonate inclusions in the sand fraction.

The air voids are usually small reaching a maximum size of approximately 7 mm. A few of these larger air voids were observed at 1.8 to 5.2 cm and 18.8 and 20.5 cm into the drill-core. The air voids contain minor amounts of colorless and white precipitates. The white precipitates are most abundant in the lower half of the pavement section.

**Section ID: 39-3801**

**State: Ohio**

**Climate: WF**

*Table 3.2.11 Mix composition of 39-3801 by linear traverse (ASTM C457).*

Coarse Aggregate	Fine Aggregate	Paste Content	Air Content
41.9 vol.%	24.9 vol.%	26.8 vol.%	6.4 vol.%

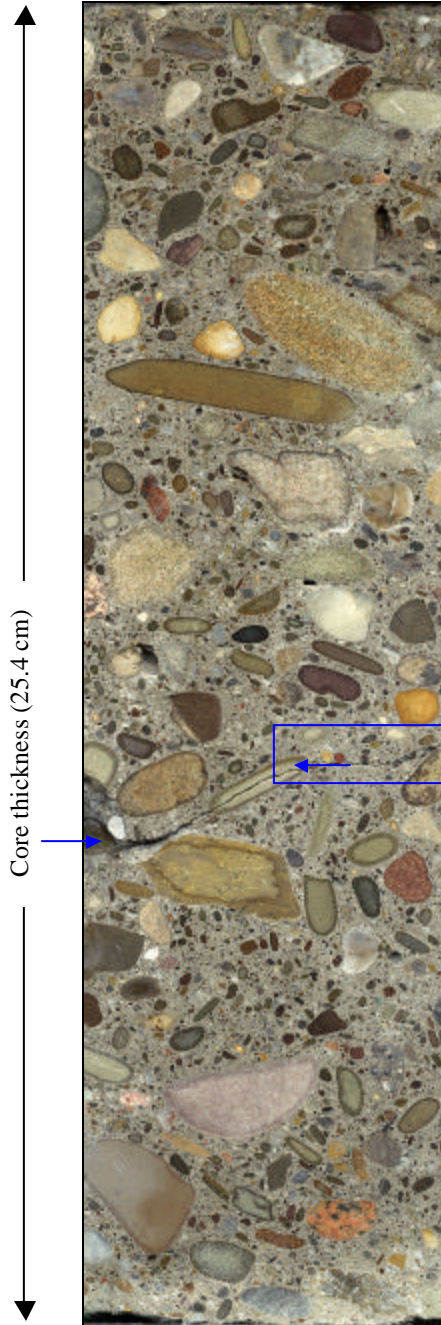


**Figure 3.2.11** Polished cross-section of pavement section 39-3801.

Pavement section 39-3801 is 25.4 cm thick and consists of rounded to well-rounded gravel embedded in a dark medium gray cement paste (figure 3.2.11). The coarse aggregates display a relatively close packing. The carbonation depth was up to 1 mm deep.

Approximately 50 volume percent of the gravel aggregates consist of dolomitic limestone and tan siltstone. The limestone may show weak reaction with 0.1M HCl. The limestone aggregates contained a dark reaction rim, up to 5 mm wide, which is related to natural weathering. The remaining 50 volume percent of the coarse aggregates consist of a mixture of igneous rocks, quartz-grains and sandstone. A few flint-like aggregates were also observed but appeared to have remained inert. The maximum recorded size of the coarse aggregates was 27 mm.

The fine aggregates consist of equal amounts of sub-rounded to well-rounded quartz-sand and dolomitic limestone. The fine limestone aggregate dominates in the fraction between 2 and 4 mm while the quartz-rich sand dominates in the size fraction below 2 mm.

Large air voids ( $\leq 11$  mm) were present below 3cm depth in the sample where a cluster of trapped air was observed at the edge of the polished slab. Below 6cm depth, the air voids normally contained white precipitates and most air voids were filled with these precipitates below 11-cm depth into the sample.

One of the slabs studied contained a horizontal open crack between 14.2- and 14.5-cm depth into the core (see arrows in figure 3.2.11). Note the wide crack in the boxed region formed after cutting and characterization of the slab. The maximum crack width ( $\ll 1$  mm) was observed around a larger air void in the sample. The crack cuts both paste and aggregates.

**Section ID: 55-3008**

**State: Wisconsin**

**Climate: WF**

*Table 3.2.12 Mix composition of 55-3008 by linear traverse (ASTM C457).*

Coarse Aggregate	Fine Aggregate	Paste Content	Air Content
51.9 vol.%	29.7 vol.%	12.2 vol.%	6.2 vol.%

Pavement section 55-3008 is 28 cm thick, the thickest section studied. The concrete is made up of angular and rounded coarse dolomite and minor gabbro aggregates in a medium gray cement paste (figure 3.2.12). The coarse aggregates display a medium to open packing with denser packing in the central part of the pavement section. Carbonation was not observed.

Some of the dolomite aggregates are relatively coarse-grained (up to ~1 mm) and are sometimes porous. A white and very porous paste often surrounds the porous aggregates. The maximum aggregate size is 43 mm while the normal coarse aggregate size appears to be around 15 mm.

The fine aggregates mainly consist of sub-rounded to well-round quartz-sand with a typical grain size of approximately 1 mm. Minor amounts of dolomite, fine-grained gabbro, and other silicate rocks are also present.

The air voids generally become larger and more abundant towards the base of the pavement section. In the polished slab, a large (~ 40-mm) and more or less horizontally oriented air void was located at intermediate depth on the backside of the slab and indicates problems with compaction.

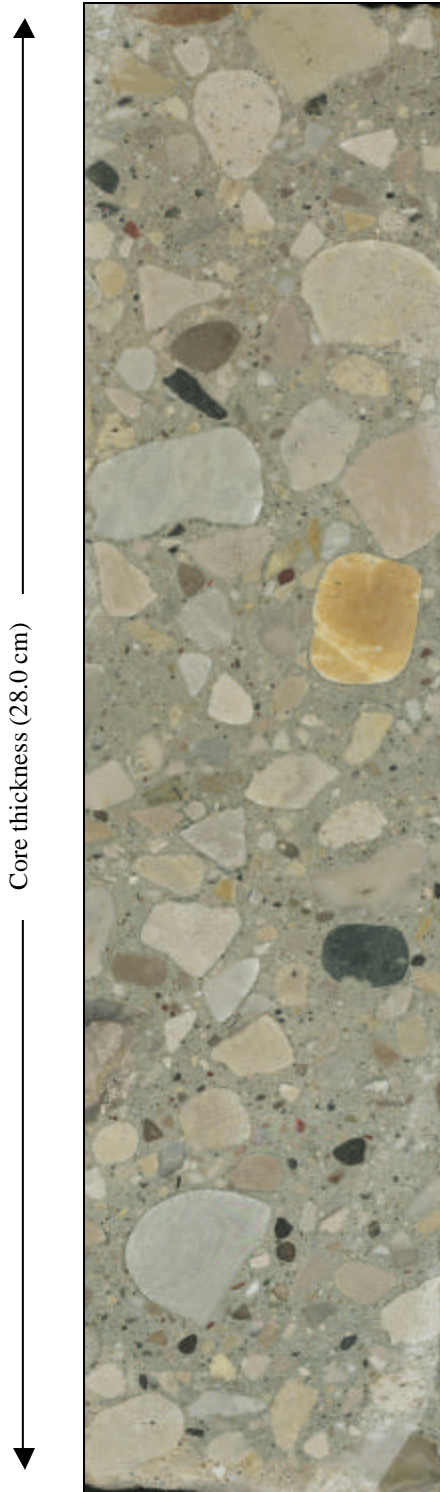


**Figure 3.2.12** Polished cross-section of pavement section 55-3008.

### 3.2.3 Petrographic Characterization of PCC Sections from the Wet-No-Freeze Region

Three samples from the WNF region were analyzed in this study. Two samples (53-3011 and 53-3812) were collected from Washington and the third sample (13-GA 1-5) was collected from Georgia. Similar to the previous samples, the concretes from the WNF region are well preserved. However, both the samples from Washington show evidence of a relatively advanced dissolution at their base.

**Section ID: 53-3011**  
**State: Washington**  
**Climate: WNF**

*Table 3.2.13 Mix composition of 53-3011 by linear traverse (ASTM C457).*

Coarse Aggregate	Fine Aggregate	Paste Content	Air Content
33.4 vol.%	34.5 vol.%	23.5 vol.%	8.6 vol.%

The core of pavement 53-3011 is 25.5 cm thick and consists of dense packed rounded to well-rounded gravel in a dark medium gray colored paste (figure 3.2.13). The carbonation depth was determined to be less than 1 mm. In the polished slab, the concrete paste showed a darker color at the top 16 to 17 cm of the core.

The composition of the gravel is complex and includes basalt, gabbro, granite, quartz-biotite, and metamorphic rocks. A few sandstone aggregates were also observed. The largest aggregate was 38 mm in diameter. A few aggregates were partially detached from the cement matrix, and there was also a tendency to the presence of higher concentrations of air voids at the interface with the coarse aggregates.

The fine aggregates consist of equal amounts of angular to rounded quartz and fine-grained mafic rock fragments. A few aggregates in the sand fraction may consist of chalcedony which have reacted during hydration of the cement paste. Some flint-aggregates may also be present.

The number of air voids appears to be relatively high. Larger air voids ( $\leq 8$  mm) were observed in the top 7 cm, as well as the lower 11 cm of the core. The air voids in the lower 8 cm of the core were frequently partially filled with white precipitates which sometimes occurred with needle-shaped morphology.

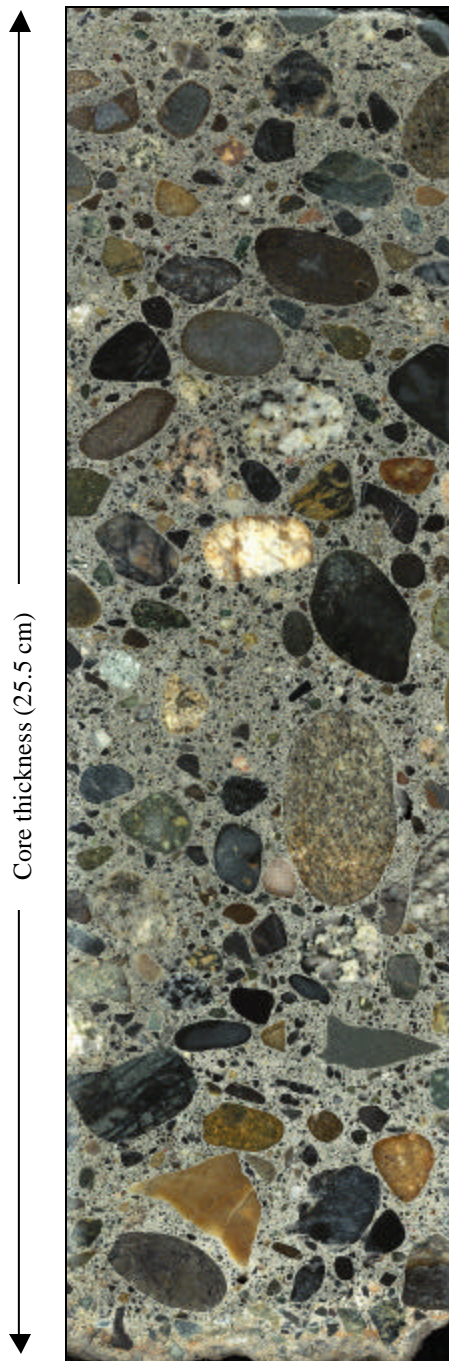
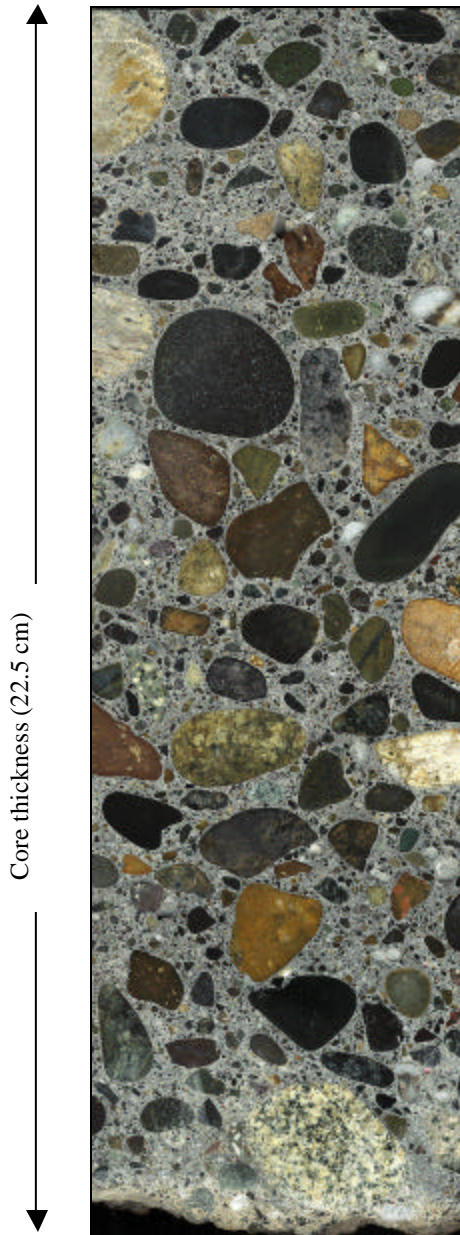


**Figure 3.2.13** Polished cross-section of pavement section 53-3011.

**Section ID: 53-3812**  
**State: Washington**  
**Climate: WNF**

*Table 3.2.14 Mix composition of 53-3812 by linear traverse (ASTM C457).*

Coarse Aggregate	Fine Aggregate	Paste Content	Air Content
41.0 vol.%	31.7 vol.%	23.9 vol.%	3.4 vol.%



Pavement section 53-3812 is 22.5 cm thick and consists of rounded to well-rounded gravel in a medium gray cement paste (figure 3.2.14). A few angular grains were also observed. The coarse aggregates are medium to close-packed. No carbonation was noted.

The coarse aggregates are up to 32 mm in diameter and consist of granite, fine-grained gabbro and well-consolidated sedimentary rocks. A light colored rim often surrounds the aggregates due to the accumulation of very fine air voids at their interface. A few aggregates were partially detached from the concrete paste.

The fine aggregates consist of rounded and angular sand with 30 to 40 volume percent quartz. The rest of the fine aggregates consist of the same material as the coarse aggregates.

The amount of large air voids in 53-3812 appears very low. Only 5 to 7 pores larger than 5 mm in diameter were observed in the cross-section. A few air voids contained precipitates.

A single “semi-vertical” crack was observed in the specimen analyzed by MDOT. The crack was observed at the top of the drill-core and ran through the paste without cutting the coarse aggregates.

*Figure 3.2.14 Polished cross-section of pavement section 53-3812.*

**Section ID: 13-GA1-5**  
**State: Georgia**  
**Climate: WNF**

Table 3.2.15 Mix composition of 13-GA1-5 by linear traverse (ASTM C457).

Coarse Aggregate	Fine Aggregate	Paste Content	Air Content
38.0 vol.%	32.0 vol.%	22.1 vol.%	7.9 vol.%



The drill-core of pavement 13-GA1-5 is 22.5 cm long and shows a concrete composed by crushed rock-fragments embedded in a pale gray cement paste (figure 3.2.15). Carbonation was not noted. The packing of the coarse aggregate appears close.

The coarse aggregates consist of a coarse-grained granitic to granodioritic rock. A few coarse aggregates of a biotite schist are also present. The largest aggregate observed was more than 36 mm in diameter.

The fine aggregates consist of the same material as the coarse aggregates. Notably, the fine aggregates also include numerous evenly dispersed biotite flakes ( $\leq 1$  mm) in addition to the crushed rock particles.

The air voids are not homogeneously distributed and the vesicles often occur in clusters. The largest air voids ( $\leq 10$  mm) are mainly observed between 9- and 15-cm depth in the sample where both spherical and angular voids are observed. The larger air voids were rarely observed at the top 9 cm of the sample. The air voids frequently contain fine-grained white and gray precipitates. According to the MTU report the precipitates in the air-void structure mainly consist of ettringite.

*Figure 3.2.15 Polished cross-section of pavement section 13-GA1-5.*

### 3.2.4. Summary of Petrographic Analysis

A summary of the petrographic analysis is shown in table 3.2.16. As reported, most of the concretes are homogeneous in their structure with some variations in their degree of packing. Most of the concretes show dense aggregate packing but a few, particularly samples 06-3021, 06-3017, and 19-3006 show open aggregate packing.

Most of the samples contain coarse aggregates of silicate rock gravel. However, the coarse aggregates in sections 19-3006, 19-3055, 27-4045, and 55-3008 from the wet freeze regions consist almost entirely of dolomitic limestone. Based on the morphology of the coarse aggregates, samples 19-3006 and 13-GA1-5 are the only concrete samples that contain considerable amounts of crushed aggregates (dolomitic limestone and granitic to granodioritic rocks, respectively). All the other concretes contain rounded to well-rounded gravel aggregates indicating that they have been subjected to some degree of natural reworking (maturation). The maximum size of the aggregates is normally below 46 mm. Sample 06-CS1, however, contains very large aggregates exceeding 76 mm. The smallest maximum aggregate size (27 mm) was observed in sample 39-3801 from the wet freeze region.

*Table 3.2.16 Summary of petrographic results.*

Climate Region	LTPP	ID	Carbonation Depth (mm)	Coarse Aggregate Type	Max Aggregate Dimension (mm)	Max Size Air void (mm)	Crack Position	Dissolution at Base
DNF	06	3017	-	gravel (mix)	46	17	N.D.	< 2 cm
	06	3021	≤15	gravel (mafic)	46	17	top, internal	negligible
	06	CS1	-	gravel (mix)	76	>15	internal	N/A
	06	CS3	≤2	gravel mix incl. dol.	45	14	top	negligible
	06	I-10	-	gravel (mix) <sup>1</sup>	44	10	N.D.	N/A
DF	53	3019	-	gravel (mafic) <sup>1</sup>	47	9	N.D.	~ 1 cm
WF	19	3006	≤4	dol. limestone <sup>2,3,4</sup>	31	6	base	very thin
	19	3055	≤3	dol. limestone <sup>4</sup>	42	11	N.D.	< 0.5 cm
	27	4054	≤4	dol. limestone <sup>4</sup>	40	7	N.D.	negligible
	39	3801	≤1	gravel + dol. limestone	27	11	internal	negligible
	55	3008	not observed	dol. limestone <sup>4</sup>	43	40	N.D.	< 1 cm
WNF	53	3011	≤	gravel (mix)	38	8	N.D.	< 2 cm
	53	3812	N.D.	gravel (mix)	32	7	top	< 2 cm
	13	GA1-5	N.D.	granite/granodiorite <sup>2</sup>	36	10	N.D.	negligible

Abbreviations: - unknown, N.D. not detected

<sup>1</sup> recycled concrete observed

<sup>2</sup> crushed rock

<sup>3</sup> relatively soft aggregates

<sup>4</sup> with minor gabbro

Despite their ages (15 to 32 years), the petrographic analysis suggests that all the pavement concretes generally are in a good state without severe deleterious reactions. The aggregates are of good quality and have mainly remained inert. A few examples, though negligible, were observed where alkali-silica reactions may have occurred. A more typical feature was the presence of reaction rims. However, the reaction rims were

not observed to have caused “problems” with respect to the performance of the concrete. In fact, the reaction rims appear to be related to weathering rather than in situ reactions.

The atmospheric weathering of the concretes results in carbonation through reactions between  $\text{CO}_2$  and the  $\text{Ca}(\text{OH})_2$  and cement hydrates in the paste. According to St. John et al. (1998), when the depth of carbonation is great enough ( $> 0.5$  mm), carbonation shrinkage is induced at the surface and microcracks develop. In the analyzed pavement concretes, the carbonation depth was normally less than 3 to 4 mm when observed. However, one sample, 06-3021, did show evidence of deep surface carbonation ( $\geq 15$  mm). Microscopic analysis of thin-sections also suggests that extensive carbonation has occurred around the air voids in 39-3801 and 13-GA1-5. In 39-3801, carbonation appears to have formed in association with microcracking in the lower half of the concrete.

Both the dolomite and silicate rock aggregates were occasionally porous. The porosity was either caused by the presence of vesicles in the volcanic aggregates, altered mineral phases, or intergranular porosity/cavities in the dolomite aggregates. However, these pore types are normally not interconnected and do not result in a high permeability. Hence, the observed aggregate porosity is not important with respect to freeze-thaw durability.



### 3.3 Presentation of Field and Laboratory Results on Concrete Properties

#### 3.3.1 Compressive Strength, Splitting Tensile Strength, and Elastic Modulus

This section presents the laboratory results for strength and elastic modulus testing on the concrete from the test sections in this study. The field compressive strengths are substantially higher than the generally required 28-day strengths for pavement concrete, which are typically in the range of 24 to 28 MPa. Tables 3.3.1 and 3.3.2 list the mechanical properties obtained in this study for the field concrete with respect to compressive strength, elastic modulus, and splitting tensile strength. The samples range from 11 to 51 years old, with an average age of 25 years at the time of testing. The average compressive strength is 49 MPa (7,105 lbf/in<sup>2</sup>), and ranges from 33 MPa (4,785 lbf/in<sup>2</sup>) for California section 06-3021, to 75 MPa (10,875 lbf/in<sup>2</sup>) for Washington section 53-3812.

**Table 3.3.1.** Measured compressive strength, split tensile strength, and elastic modulus for cored samples from each of the test pavement sections of the DNF and DF regions.

*Note, values in bold are the average values for each test section.*

Region	Database		Measured Compressive Strength		h/d <sup>1</sup>	Corrected Compressive Strength		Measured Split Tensile Strength		Measured Elastic Modulus	
	State ID	Section ID	MPa	lbf/in <sup>2</sup>		MPa	lbf/in <sup>2</sup>	Mpa	lbf/in <sup>2</sup>	MPa	lbf/in <sup>2</sup>
DNF	06	3017	38.8	5633	1.40	36.8	5340	3.64	528	26821	3889000
			40.3	5842	1.30	38.1	5527	3.72	539	26666	3866500
			42.4	6155	1.34	39.9	5791	3.35	486	24117	3497000
			<b>40.5</b>	<b>5877</b>		<b>38.3</b>	<b>5552</b>	<b>3.57</b>	<b>518</b>	<b>25868</b>	<b>3750833</b>
	06	3021	34.0	4930	1.41	32.3	4680	3.15	457	22686	3289500
			34.5	5007	1.38	32.7	4735	3.77	547	25769	3736500
			36.7	5320	1.32	34.5	5003	3.39	492	22686	3289500
			<b>35.1</b>	<b>5086</b>		<b>33.1</b>	<b>4806</b>	<b>3.44</b>	<b>499</b>	<b>23714</b>	<b>3438500</b>
	06	7456	36.7	5317	1.88	35.9	5211	3.63	526	25710	3728000
			37.7	5472	1.85	37.0	5363	2.93	425	24086	3492500
			<b>37.2</b>	<b>5395</b>		<b>36.5</b>	<b>5287</b>	<b>3.28</b>	<b>475</b>	<b>24898</b>	<b>3610250</b>
	06	CS1	46.9	6807	1.45	44.8	6494	3.48	505	32634	4732000
			47.8	6937	1.40	45.4	6576			30224	4382500
			<b>47.4</b>	<b>6872</b>		<b>45.1</b>	<b>6535</b>	<b>3.48</b>	<b>505</b>	<b>31429</b>	<b>4557250</b>
	06	CS3	56.1	8137	1.34	52.8	7655	4.18	606	33738	4892000
			67.9	9846	1.36	64.0	9287	3.36	487	35621	5165000
			<b>62.0</b>	<b>8992</b>		<b>58.4</b>	<b>8471</b>	<b>3.77</b>	<b>547</b>	<b>34679</b>	<b>5028500</b>
06	I-10	39.4	5711	1.46	37.6	5455	4.30	623	28321	4106500	
		<b>39.4</b>	<b>5711</b>		<b>37.6</b>	<b>5455</b>	<b>4.00</b>	<b>580</b>	<b>28321</b>	<b>4106500</b>	
DF	53	3019	52.3	7589	1.70	51.1	7407	4.21	611	39086	5667500
			61.9	8970	1.65	60.1	8719	3.95	573	42017	6092500
			<b>57.1</b>	<b>8280</b>		<b>55.6</b>	<b>8063</b>	<b>4.26</b>	<b>618</b>	<b>40552</b>	<b>5880000</b>

<sup>1</sup> h/d is the height to diameter ratio used for strength correction according to ASTM specifications

**Table 3.3.2. Measured compressive strength, split tensile strength, and elastic modulus for cored samples from each of the test pavement sections of the WNF and WF regions.**

*Note, values in bold are the average values for each test section.*

Region	Database		Measured Compressive Strength		h/d <sup>1</sup>	Corrected Compressive Strength		Measured Split Tensile Strength		Measured Elastic Modulus	
	State ID	Section ID	MPa	lbf/in <sup>2</sup>		MPa	lbf/in <sup>2</sup>	MPa	lbf/in <sup>2</sup>	MPa	lbf/in <sup>2</sup>
WF	19	3006	49.6	7199	1.40	47.1	6825	3.97	576	32469	4708000
			50.2	7276	1.49	48.1	6976	3.20	464	30621	4440000
			44.8	6494	1.36	42.2	6125	3.34	485	31607	4583000
			<b>48.2</b>	<b>6990</b>		<b>45.8</b>	<b>6642</b>	<b>3.51</b>	<b>508</b>	<b>31566</b>	<b>4577000</b>
	19	3055	43.7	6338	1.47	41.8	6062	3.61	523	25510	3699000
			42.6	6181	1.68	41.5	6023	2.22 <sup>2</sup>	322	26007	3771000
			<b>43.2</b>	<b>6260</b>		<b>41.7</b>	<b>6042</b>	<b>2.91</b>	<b>423</b>	<b>25759</b>	<b>3735000</b>
	27	4054	61.5	8918	1.50	59.0	8561	3.32	481	40614	5889000
			50.2	7276	1.52	48.3	6997	3.44	499	37969	5505500
			57.8	8377	1.59	55.9	8102	4.31	625	38559	5591000
			<b>56.5</b>	<b>8190</b>		<b>54.4</b>	<b>7887</b>	<b>3.69</b>	<b>535</b>	<b>39047</b>	<b>5661833</b>
	39	3801	51.1	7406	1.50	49.0	7110	3.39	491	24779	3593000
			49.6	7197	1.52	47.7	6921	3.90	566	25041	3631000
			41.5	6023	1.43	39.5	5731	3.89	564	25917	3758000
			<b>47.4</b>	<b>6875</b>		<b>45.4</b>	<b>6587</b>	<b>3.73</b>	<b>540</b>	<b>25246</b>	<b>3660667</b>
55	3008	62.6	9074	1.75	61.3	8893	4.62	670	42862	6215000	
		59.9	8684	1.83	59.1	8566	4.54	658	45090	6538000	
		65.8	9544	1.68	64.1	9300	4.33	628	46538	6748000	
		<b>62.8</b>	<b>9101</b>		<b>61.5</b>	<b>8919</b>	<b>4.50</b>	<b>652</b>	<b>44830</b>	<b>6500333</b>	
WNF	53	3011	62.2	9023	1.55	60.0	8698	3.71	538	40310	5845000
			61.5	8918	1.55	59.3	8597	3.97	575	43179	6261000
			<b>61.9</b>	<b>8971</b>		<b>59.6</b>	<b>8648</b>	<b>3.84</b>	<b>557</b>	<b>41745</b>	<b>6053000</b>
	53	3812	76.1	11030	1.56	73.4	10642	4.05	588	49007	7106000
			81.3	11790	1.36	76.7	11120	4.75	689	44855	6504000
			<b>78.7</b>	<b>11410</b>		<b>75.0</b>	<b>10881</b>	<b>4.40</b>	<b>638</b>	<b>46931</b>	<b>6805000</b>
	13	GA1-5	33.1	4798	1.40	31.4	4549	3.27	474		
			47.1	6833	1.66	43.7	6341	2.72 <sup>2</sup>	394	28366	4113000
			36.7	5320	1.48	35.1	5094	3.00	435	21614	3134000
		<b>39.0</b>	<b>5650</b>		<b>36.7</b>	<b>5328</b>	<b>3.00</b>	<b>434</b>	<b>24990</b>	<b>3623500</b>	

<sup>1</sup> h/d is the height to diameter ratio used for strength correction according to ASTM specifications

<sup>2</sup> data point in question

Overall, the test results for mechanical properties from this study and LTPP are in good agreement, as seen in table 3.3.3. However, the LTPP database does in general show higher compressive strength values by an average of 17 percent. This is likely related in part to the use of smaller specimen sizes (100- by 200-mm cores) in the LTPP database. This study uses 150- by 200- to 250-mm cores with an additional correction for height-to-diameter ratio. Specimen size affects the measured strength, with smaller specimens yielding higher strength (e.g. Price, 1951).

**Table 3.3.3** Compressive strength, splitting tensile strength, and elastic modulus for each test section. (Data is from this study and from the LTPP database (DataPave 97). Values reported are averages of all specimens tested for each test section.)

Climate Region	LTPP		Section Age		Compressive Strength			Elastic Modulus			Split. Tensile Strength		
	State ID	Section ID	LTPP (Yrs)	This Study (Yrs)	LTPP (MPa)	This Study (MPa)	% Diff.	LTPP (MPa)	This Study (MPa)	% Diff.	LTPP (MPa)	This Study (MPa)	% Diff.
DNF	06	3017	19	20	44	38	13	28276	25868	9	5.0	3.7	26
	06	3021	18	24	44	33	25	21034	23714	-13	5.1	3.5	32
	06	7456	20	26	50	37	26	29138	24898	15	5.7	3.3	43
	06	CS1	20	26		45			31429			3.5	
	06	CS3	20	26		58			34679			4.2	
	06	I-10		51		38			28321			4.3	
DF	53	3019	6	11	64	56	13	34138	40552	-19	6.2	4.2	32
WF	19	3006	19	22	58	46	22	31552	31566	0	3.4	3.5	-3
	19	3055		28	59	42	29	23966	25759	-7	3.9	2.8	28
	27	4054	19	25	57	54	5	38276	39047	-2	4.0	3.7	7
	39	3801	11	13	59	45	23	25862	25246	2	3.2	3.7	-15
	55	3008	19	22	72	62	14	46897	44830	4	4.7	4.5	5
WNF	53	3011	15	20		60		36379	41745	-15	7.0	3.8	45
	53	3812	27	33	79	75	5	45690	46931	-3	6.2	4.4	28
	13	GA1-5/6		26		37			24990			3.0	
<b>Avg</b>			18	25	59	48	18	32837	32638	-3	4.9	3.7	21
<b>Max</b>			27	51	79	75	29	46897	46931	9	7.0	4.5	45
<b>Min</b>			6	11	44	33	5	21034	23714	-19	3.2	2.8	-15

### 3.3.2 Fracture Energy

Fracture energy was measured in this study from test beams from four California test sections. The beams were tested according to the RILEM 50-FCM test procedure as was described in sections 2.4 and 5.5. The results are listed in table 3.3.4.

The beams were cut directly from the insitu pavement slabs. Thus, the beam height is the slab thickness. Because the slabs from the different test sections were of different thickness, the notch-to-depth ratio in the test beams varied somewhat. This variation is taken into account when calculating the fracture energy. The variation of the fracture energy values within each site is within the expected variation for fracture energy beam testing. See section 5.5.

The laboratory mixes used for development of recommendations were designed to investigate the effect of coarse aggregate type and size using the fracture energy test. The results from the laboratory mixes are also discussed in section 5.5. Considering the laboratory mix results, the fracture energy results obtained from the field are what would be expected for highway concretes containing gravel as coarse aggregate. This observation is important because fracture energy results are not available in the LTPP database for comparison.

*Table 3.3.4 Summary of fracture energy testing results from the tested study sections.*

Climate Region	LTPP		Specimen	Fracture Energy N/m	Notch to Depth Ratio
	State	Section			
DNF	06	3017	#1	250	0.43
			#2	175	0.44
			#3	249	0.43
			<b>Mean</b>	<b>225</b>	<b>0.43</b>
	06	3021	#1	179	0.42
			#2	241	0.40
			#3	184	0.42
			<b>Mean</b>	<b>202</b>	<b>0.41</b>
	06	CS3	#1	286	0.47
			#2	284	0.45
			<b>Mean</b>	<b>285</b>	<b>0.46</b>
	06	I-10	#1	199	0.37
			#2	261	0.35
			<b>Mean</b>	<b>230</b>	<b>0.36</b>

### 3.3.3 Transport Properties

Permeability is not determined in the LTPP database, so all data reported here was measured in this study, using various test methods. Chloride ion penetration resistance and air permeability are measured at three depths within the concrete. For the Rapid Chloride Permeability Test (RCPT), the top sample is taken 12 mm beneath the concrete surface, extending 50 mm below that. The middle and bottom samples are taken successively below that one. Air permeability is measured at approximately 12 mm beneath the surface for the top reading. Middle and bottom readings are taken at approximately 100 and 200 mm beneath the surface where possible. Water permeability readings are taken at two depths, roughly 30 to 40 mm below the surface for the top reading and 130 to 140 mm below the surface for the bottom reading. Water sorption tests were performed on two 38 mm thick samples, one at the pavement surface, and one immediately beneath the first sample. The transport property test methods have been described in detail in chapter 2.

RCPT results were highly repeatable for the concretes that were studied. On the other hand, the water permeability results were questionable for a number of the samples due to observed leaking during the test. It was not clear whether the cracks were caused by the test or had been present beforehand. The questionable data points have not been reported. While there is some variability in the air permeability results this is expected. Air permeability values can span five orders of magnitude so only broad classifications are generally made. Water sorption is perhaps the simplest test procedure, and it yields very useful results, as will be discussed further in Chapters 5 and 6. Tables 3.3.5-3.3.10 show the results from the various tests.

**Table 3.3.5** Rapid Chloride Permeability Test results for the DNF and DF climate regions. Results are for successive test specimens cut with increasing depth in each core sample tested.

Climate	Section ID		State	Sample	RCPT Results (Coulombs)						
	State	Section			1st (Top)	2nd from Top	3rd from Top	4th (Bottom)			
DNF	6	3017	California	1	6680	4146	1564	--			
				2	6062	2555	1077	--			
				3	4558	3526	1857	--			
				4	4918	4361	3485	--			
				<b>AVG</b>	<b>5555</b>	<b>3647</b>	<b>1996</b>	--			
				<b>STDev</b>	<b>987</b>	<b>810</b>	<b>1044</b>	--			
	6	3021	California	1	4720	5854	4173	--			
				2	6563	5132	5638	--			
				3	3318	3617	2067	--			
				4	3843	3878	2637	--			
				<b>AVG</b>	<b>4611</b>	<b>4620</b>	<b>3629</b>	--			
				<b>STDev</b>	<b>1424</b>	<b>1055</b>	<b>1608</b>	--			
	6	7456	California	1	2324	3017	990	921			
				2	3163	2046	1389	1593			
				<b>AVG</b>	<b>2744</b>	<b>2532</b>	<b>1190</b>	<b>1257</b>			
				<b>STDev</b>	<b>593</b>	<b>687</b>	<b>282</b>	<b>475</b>			
				6	CS1	California	1	1719	1916	387	--
							2	2191	1862	673	--
	3	1999	1133				639	291			
	<b>AVG</b>	<b>1970</b>	<b>1637</b>				<b>566</b>	<b>291</b>			
	<b>STDev</b>	<b>237</b>	<b>437</b>	<b>156</b>	--						
	6	CS3	California	1	1406	751	530	--			
				2	1197	971	444	--			
				3	1433	667	323	--			
<b>AVG</b>				<b>1345</b>	<b>796</b>	<b>432</b>	--				
<b>STDev</b>	<b>129</b>	<b>157</b>	<b>104</b>	--							
6	I-10	California	1	3526	3187	1096	--				
			2	3891	2886	1508	--				
			3	3890	3480	1056	--				
			<b>AVG</b>	<b>3769</b>	<b>3184</b>	<b>1220</b>	--				
<b>STDev</b>	<b>210</b>	<b>297</b>	<b>250</b>	--							
DF	53	3019	Washington	1	557	105	71	29			
				2	287	76	106	56			
				3	356	--	--	215			
				<b>AVG</b>	<b>400</b>	<b>91</b>	<b>89</b>	<b>100</b>			
				<b>STDev</b>	<b>140</b>	<b>21</b>	<b>25</b>	<b>101</b>			

**Table 3.3.6** Rapid Chloride Permeability Test results for the WF and WNF climate regions. Results are for successive test specimens cut with increasing depth in each core sample tested.

Climate	Section ID		State	Sample	RCPT Results (Coulombs)			
	State	Section			1st (Top)	2nd from Top	3rd from Top	4th (Bottom)
WF	19	3006	Iowa	1	2497	1237	785	--
				2	1633	865	577	--
				3	1855	1744	--	--
				<b>AVG</b>	<b>1995</b>	<b>1282</b>	<b>681</b>	<b>--</b>
				<b>STDev</b>	<b>449</b>	<b>441</b>	<b>147</b>	<b>--</b>
	19	3055	Iowa	1	1656	1023	1242	973
				2	4203 <sup>1</sup>	1829	1850	2338
				<b>AVG</b>	<b>1656</b>	<b>1426</b>	<b>1546</b>	<b>1656</b>
				<b>STDev</b>	<b>--</b>	<b>570</b>	<b>430</b>	<b>965</b>
	27	4054	Minnesota	1	1184	725	766	229
				2	3782 <sup>1</sup>	810	592	445
				<b>AVG</b>	<b>1184</b>	<b>768</b>	<b>679</b>	<b>337</b>
				<b>STDev</b>	<b>--</b>	<b>60</b>	<b>123</b>	<b>153</b>
39	3801	Ohio	1	1802	1533	790	709	
			2	1207	1217	1792	947	
			<b>AVG</b>	<b>1505</b>	<b>1375</b>	<b>1291</b>	<b>828</b>	
			<b>STDev</b>	<b>421</b>	<b>223</b>	<b>709</b>	<b>168</b>	
55	3008	Wisconsin	1	225	288	312	324	
			<b>AVG</b>	<b>225</b>	<b>288</b>	<b>312</b>	<b>324</b>	
			<b>STDev</b>	<b>--</b>	<b>--</b>	<b>--</b>	<b>--</b>	
WNF	53	3011	Washington	1	652	390	--	251
				2	606	288	301	456
				3	779	363	442	279
				4	1112	500	351	283
				<b>AVG</b>	<b>787</b>	<b>385</b>	<b>365</b>	<b>317</b>
	53	3812	Washington	1	448	530	345	--
				2	561	354	318	--
				3	443	214	208	--
				4	257	237	202	--
				<b>AVG</b>	<b>427</b>	<b>334</b>	<b>268</b>	<b>--</b>
	13	GA1-5	Georgia	1	7030	2349	1653	--
		13	GA1-6	Georgia	1	6825	6268	4248
				<b>AVG</b>	<b>6928</b>	<b>4309</b>	<b>2951</b>	<b>4157</b>
			<b>STDev</b>	<b>145</b>	<b>2771</b>	<b>1835</b>	<b>--</b>	

<sup>1</sup> Data point in question.

**Table 3.3.7 Air Permeability Test results for the DNF and DF climate regions.**

<b>Air Permeability</b>							
<b>Climate</b>	<b>State</b>	<b>Section</b>	<b>Measurement Location</b>	<b>Air Permeability Kt (10-16 m<sup>2</sup>)</b>	<b>Penetration Depth L (mm)</b>	<b>Electrical Resistance (kohm cm)</b>	<b>Permeability Class</b>
DNF	06	3017	Top	1.032	53.1	--	Bad
			Middle	0.175	28.5	135	Normal
			Middle	0.200	30.6	155	Normal
			Bottom	0.015	8.5	184	Good
	06	3021	Top	4.426	77.6	--	Bad
			Middle	1.047	53.4	293	Bad
			Middle	0.134	25.0	223	Normal
			Bottom	0.172	28.3	310	Normal
	06	CS1	No Test				
	06	CS3	No Test				
	06	I-10	Top	1.632	56.4	--	Bad
			Middle	0.449	44.9	307	Normal
			Middle	0.599	46.9	216	Normal
Bottom			0.086	20.1	207	Good	
DF	53	3019	Top	0.893	51.0	--	Normal
			Middle	0.016	8.7	--	Good
			Middle	0.038	13.4	560	Good
			Bottom	0.017	8.9	--	Good

**Table 3.3.8 Air Permeability Test results for the WF and WNF climate regions.**

<b>Air Permeability</b>						
<b>Climate Region</b>	<b>State Section</b>	<b>Measurement Location</b>	<b>Air Permeability Kt (<math>10^{-16} \text{ m}^2</math>)</b>	<b>Penetration Depth L (mm)</b>	<b>Electrical Resistance (kohm cm)</b>	<b>Permeability Class</b>
WF	19 3006	Top	0.693	47.9	243	Normal
		Middle	0.308	37.9	177	Normal
		Middle	0.013	7.8	176	Good
		Bottom	0.009	6.3	195	Very Good
	19 3055	Top	0.033	12.5	77	Good
		Middle	0.067	17.7	63	Good
		Middle	0.107	22.3	52	Normal
		Bottom	0.114	23.0	54	Normal
	27 4054	Top	0.125	24.1	116	Normal
		Middle	0.070	18.0	140	Good
		Middle	0.088	20.3	113	Good
		Bottom	0.046	14.6	123	Good
	39 3801	Top	0.086	20.0	92	Good
		Middle	0.026	11.1	61	Good
		Middle	0.039	13.5	56	Good
		Bottom	0.008	6.3	56	Very Good
55 3008	Top	0.042	14.0	169	Good	
	Middle	0.019	9.4	179	Good	
	Middle	0.037	13.1	150	Good	
	Bottom	0.034	12.6	116	Good	
WNF	53 3011	Top	7.103	91.1	210	Bad
		Middle	0.006	5.5	--	Very Good
		Middle	0.001	2.4	151	Very Good
		Bottom	0.029	11.6	--	Good
	53 3812	Top	0.22	32.1	313	Normal
		Middle	0.017	9	212	Good
		Middle	0.042	14	205	Good
		Bottom	0.02	9.8	214	Good
	13 GA1-5	Top	0.399	43.2	60	Normal
		Middle	0.039	13.6	34	Good
		Middle	0.595	46.9	58	Normal
		Bottom	0.172	28.4	69	Normal



**Table 3.3.9** Water permeability test results.

Climate Region	LTPP		Water Permeability (cm/secx10 <sup>-11</sup> )	
	State ID	Section ID	Top	Bottom
DNF	06	3017	303.4	--
	06	3021	--	--
	06	7456	--	--
	06	CS1	--	--
	06	CS3	--	--
	06	I-10	--	--
DF	53	3019	56.1	--
WF	19	3006	117.2	81.0
	19	3055	--	50.4
	27	4054	53.6	--
	39	3801	--	38.2
	55	3008	48.7	--
WNF	53	3011	42.9	--
	53	3812	16.9	--
	13	GA1-5	155.1	99.3

**Table 3.3.10** Water absorption rate results from water sorption test.

Climate Region	Test Section ID	Absorption Rate	
		Top Sample kg/m <sup>2</sup> /h <sup>0.5</sup>	2nd Sample kg/m <sup>2</sup> /h <sup>0.5</sup>
DNF	06-3017	0.82	0.79
	06-3021	0.93	1.48
	06-7456	0.91	0.81
	06-CS1	0.85	0.71
	06-CS3	0.47	0.40
	06-I10	0.88	0.76
DF	53-3019	0.38	0.27
WF	19-3006	0.56	0.59
	19-3055	0.71	0.82
	27-4054	0.72	0.72
	39-3801	0.55	0.57
	55-3008	0.43	0.41
WNF	53-3011	0.40	0.38
	53-3812	0.40	0.51
	13-GA1-5	1.30	1.47

### 3.3.4 Coefficient of Thermal Expansion

Coefficient of thermal expansion is not complete in the LTPP database. Thus, all data presented is from field cores in this study. The coefficient of thermal expansion was tested according to a recommended procedure from FHWA as described in chapter 2. The procedure was modified for continuous measurements of temperature and deformations of the concrete for improved accuracy.

The values measured in this study fall within the acceptable range for concrete coefficient of thermal expansion, as seen in table 3.3.11. The concretes have a relatively narrow range of values. Results are measured against a stainless steel reference bar to ensure testing accuracy. The coefficient of thermal expansion is averaged from the value obtained with increasing temperature and the value obtained from decreasing temperature. Note that the coefficient of thermal expansion may differ 10 to 20 percent between two temperature cycles.

**Table 3.3.11.** Measured coefficient of thermal expansion for cored samples from each of the tested pavement sections of this study.

Climate Region	LTPP		Specimen ID	$\alpha$ (10-50 C) (*10 <sup>-6</sup> )	$\alpha$ (10-50 C) ref. (*10 <sup>-6</sup> )	$\alpha$ (50-10 C) (*10 <sup>-6</sup> )	$\alpha$ (50-10 C) ref. (*10 <sup>-6</sup> )	Average $\alpha$ (*10 <sup>-6</sup> )
	State ID	Section ID						
DNF	06	3017	-	-	-	-	-	NA
	06	3021	-	-	-	-	-	NA
	06	7456	C7	9.1	-	10.5	-	9.8
			C8	9.2	-	11.3	-	10.3
	06	CS1	C4	9.9	17.1	9.7	16.2	9.8
	06	CS3	C19	13.1	16.3	14.2	16.4	13.7
	06	I-10	C6	8.2	17.3	8.5	17.6	8.4
DNF Region Average: 10.4								
DF	53	3019	C3	9.8	17.4	8.5	17.4	9.2
			C8	8.4	16.9	8.6	17.4	8.5
DF Region Average: 8.9								
WF	19	3006	-	-	-	-	-	NA
	19	3055	C11	9.8	-	9.7	-	9.8
			C19	8.3	-	8.7	-	8.5
	27	4054	C4	9.1	-	8.4	-	8.8
			C5	9.7	16.5	9.3	16.9	9.5
	39	3801	C3	11.3	17.5	11.9	17.9	11.6
	55	3008	C12	9.7	17.1	9.5	-	9.6
C15			8.8	18.0	8.8	19.0	8.8	
WF Region Average: 9.5								
WNF	53	3011	-	-	-	-	-	
	53	3812	C17	9.9	17.1	8.3	17.2	9.1
			C10	13.3	17.3	12.5	16.6	12.9 <sup>1</sup>
	13	GA1-5	C14	9.5	17.0	8.5	16.3	9.0
WNF Region Average: 9.1								

<sup>1</sup> Data point in question